PETROGRAPHY AND GEOCHRONOLOGY OF BASIC AND ULTRABASIC INCLUSIONS FROM KIMBERLITES OF RILEY COUNTY, KANSAS

by 4589

MICHAEL JOSEPH WOODS

B.A., University of Pennsylvania, 1964

A MASTER'S THESIS

submitted in partial fulfillment of the

requirements for the degree

MASTER OF SCIENCE

Department of Geology and Geography

KANSAS STATE UNIVERSITY
Manhattan, Kansas

1970

Approved by:

Douglas L. Brookins

Major Professor

TABLE OF CONTENTS

THIS BOOK CONTAINS NUMEROUS PICTURES THAT ARE ATTACHED TO DOCUMENTS CROOKED.

THIS IS AS RECEIVED FROM CUSTOMER.

THIS BOOK CONTAINS NUMEROUS PAGES WITH DIAGRAMS THAT ARE CROOKED COMPARED TO THE REST OF THE INFORMATION ON THE PAGE.

THIS IS AS RECEIVED FROM CUSTOMER.

LIST OF ILLUSTRATIONS

Figure

LIST OF TABLES

INTRODUCTION

Basic and ultrabasic nodules in kimberlitic and peridotitic intrusions are considered by many to provide invaluable data regarding the composition of the earth's mantle and lower crust, and to suggest the processes by which basaltic magmas are formed.

This investigation deals with several nodules from the Stockdale kimberlite pipe of Riley County, Kansas. The purposes of the study are to (1) provide complete petrographic descriptions of these nodules, (2) provide Rb-Sr geochronologic data, and (3) attempt interpretations of the origins and histories of the samples.

Occurrences of Inclusions

Inclusions within basic or ultrabasic lavas and diatremes may be either accidental or cognate. Accidental inclusions (which may be termed xenoliths) include fragments of the basement complex, fragments of host rock into which the diatreme is injected, or fragments of overlying formations which have been eroded away since the time of injection.

In a strict sense, the term "cognate inclusion" refers to material which is generically related to the host magma, generally as a crystal cumulate. In practice, however, some authors use it in reference to any ultrabasic inclusion belonging to the granulite or eclogite facies. Because some inclusions are believed accidental, whereas others are considered cognate (sensu strictu), such usage has led to some confusion in the literature.

Many authors get around this difficulty by using the expression "ultrabasic nodule"; this practice is adopted here.

Ultrabasic nodules and crustal xenoliths may be found in flows, pyroclastics, or in hypabyssal intrusions. If the bulk analyses of ultrabasic nodule-bearing magmas are plotted in the "normative tetrahedron" (quartz-albite-hypersthene-olivine-diopside-nepheline) of Yoder and Tilley (1962), they fall within the undersaturated region; the only apparent exceptions being three olivine-bearing nodules from a Hawaiian olivine tholeiite (White, 1966). Gabbroic inclusions occur within both alkali basalts and silica-saturated lavas.

Wyllie (1967) distinguished three environments in which ultrabasic nodules may be found: alkali olivine basalt, alkali ultrabasic lavas (commonly in ring complexes) and kimberlites. There appear to be no particular nodule compositions, with the exception of eclogites, restricted to any specific magmatic environment. By far the most abundant composition is that of lherzolite, which is even in the Hawaiian olivine tholeiite (White, 1966). Local conditions may range widely, however, and it is remarkable that not a single grain of olivine has been identified with certainty in any of the Riley County nodules.

White (1966) found that Hawaiian nodules occur preferentially in two groups, with lherzolites generally being found in extremely undersaturated alkali basalts such as olivine nephelinite and nepheline basanite, while dunite, wehrlite, and clinopyroxenite favor moderately undersaturated alkali basalt such as

olivine basalt, hawaiite, and ankaramite. This pattern is repeated elsewhere as, for example, on Iki Island, Japan, where dunite, peridotite, and pyroxenite are found in alkali basalt, while lherzolite group assemblages are absent (Aoki, 1968). On the other hand, Aoki and Kushiro(1968) report both groups in the basanites of Dreiser Weiher, Eifel, Germany, which emphasizes that each group is not restricted to any specific environment.

Eclogite nodules have been reported from a very few varieties of host rocks. They occur principally in kimberlites. Not all kimberlites contain them, however. Other occurrences are in basanite (Green, 1966) and alkali olivine basalt (O'Hara, 1969). The last suggests that their restricted occurrence may largely be a function of general scarcity.

Ultrabasic Nodules in Kimberlites

Very few published data are available on the ultrabasic inclusions in kimberlites. This is remarkable inasmuch as kimberlites are generally very rich in inclusions, often of a very wide variety. The Garnet Ridge diatremes of Arizona have been reported by Watson and Morton (1968) to contain amphibolites, pyroxene granulites, peridotites, serpentine-actinolite-carbonate rocks, pyroxenites, eclogites, and other types. The kimberlites of Basutoland contain lherzolite, garnet wehrlite, saxonite, pyroxenite, garnet pyroxenite, and eclogite (Nixon et al, 1963). A general summary of the occurrence of cognate nodules in kimberlites is given by O'Hara (1967).

So far, only a very limited variety of nodule species has been found in the Riley County kimberlites. Known specimens include gabbro, metagabbro, spinel granulite, garnet granulite, pyroxenite, and eclogite. In addition to the nodules there are, of course, crustal xenoliths of such rocks as norite and diorite.

Because the ultrabasic nodules in kimberlites are similar to nodules found in other ultrabasic intrusions, it is assumed that the processes responsible for their formation are similar in the different environments. There is evidence for this in the fact that the kimberlites themselves may be related generically to other ultrabasic intrusive magmas. O'Hara (1968) has suggested that kimberlites and olivine melilites may represent the products of eclogite-fractionated magmas under different intrusion temperatures, while White (1966) has reported nodules of both (his) extremely undersaturated and moderately undersaturated groups in Hawaiian olivine melilite. It therefore seems appropriate to review the theories of nodule formation without restricting the discussion to only those varieties abundant in kimberlites. Some of the latest interpretations are presented in the following section.

ORIGIN OF NODULES - LITERATURE REVIEW

Theories for the origin of ultrabasic nodules may for convenience be divided into three categories, holding that they are: (1) xenoliths of upper mantle material, (2) crystalline residua of the upper mantle after partial melting has produced their host

magma, and (3) crystal accumulates from the rising magma.

Interpretations (1) ans (2) are generally confined to olivine rich nodules in which "lherzolite" is generally used. By strict definition, this is a peridotite containing diallage and orthopyroxene in approximately equal amounts, and it is obvious that many authors use this term for other varieties of peridotite, including, in some cases, garnet-bearing varieties. I will use the term "lherzolite" in the following discussion, but the above qualification should be borne in mind.

White (1966) after considering such factors as lack of iron enrichment, constancy of silicate phase composition, and absence of poikilitic pyroxenes, concluded that the Hawaiian lherzolites represent either residua of fusion in the upper mantle or fragments of infusible portions. Green and Ringwood (1967) showed that the estimated equilibration temperature of under 1000° C and the compositions of lherzolitic pyroxenes and spinel are inconsistent with liquidus equilibrium with a basaltic liquid, and conclude that lherzolite nodules are either xenoliths of residual mantle peridotite after basalt has been removed, or fragments of mantle from which only "incompatible elements" (U, Pb, Th, K, Rb, Sr, Zr, etc.) have been removed. Kleeman et al (1969) demonstrated that lherzolite nodules in basanites of western Victoria were formed out of equilibrium with basaltic liquid, basing their argument upon uranium partition coefficients of secondary phases. They concluded that the xenoliths are accidental fragments of an inhomogeneous upper mantle. The same conclusion was drawn by

Cooper and Green (1969) after demonstrating that the lherzolites have lower Pb^{206}/Pb^{204} values than the host basalt. Leggo and Hutchison (1968) have shown that the Sr^{87}/Sr^{86} values of lherzolite nodules from the Massif Central of France differ from those of the host basalt, and concluded that the nodules must be accidental mantle fragments. Aoki and Kushiro (1968) favored a similar origin for lherzolite inclusions from Eifel, Germany, based upon the low TiO_2 and Fe_2O_3 and high Cr_2O_3 content of their clinopyroxenes. Laughlin et al (1970) have shown that some lherzolites from Bandera Crater, New Mexico, are not in equilibrium with their host basalts on the basis of Sr isotopic work and probably, therefore, represent upper mantle material.

Nagasawa (1969) demonstrated that rare earth partitioning between nodule and host for four different intrusions did not correspond to calculated partition coefficients. He concluded that the nodules have no genetic relationship to their host rocks, but are fragments of deep-seated peridotites which had once supplied magmas. His samples were from an alkali olivine basalt, a nephelenite tuff, a basanite lava, and an alkali olivine tuff with high Al_2O_3 and K_2O content. Griffin and Murthy (1968) compared the K, Rb, Sr, and Ba contents of individual minerals from several eclogite nodules with the values obtained for their host rocks (kimberlite and alkalic basalt). They proposed a model in which solid fragments are incorporated as xenoliths, while more extensive melting produces oceanic-type tholeiites which incorporate individual minerals from the solid mantle

ILLEGIBLE DOCUMENT

THE FOLLOWING DOCUMENT(S) IS OF POOR LEGIBILITY IN THE ORIGINAL

THIS IS THE BEST COPY AVAILABLE

as xenocrysts.

The mechanism of crystal accumulation from magma has been proposed for a variety of nodule species. Green (1966) concluded that pyroxenite and garnet pyroxenite (eclogite) inclusions from Salt Lake Crater, Hawaii, crystallized as clinopyroxenite in a range of 13-18 kilibars pressure, with subsequent cooling at some constant pressure causing garnet exsolution. Green and Ringwood (1967) cited exsolution textures in pyroxenite nodules from western Victoria as evidence that they crystallized as cumulate phases. In a study of wehrlites and clinopyroxenites from the Dreiser Weiher basanites, Aoki and Kushiro (1968) showed that the clinopyroxenes from these nodules are rich in acmite, and pointed out that this is typical of pyroxenes from alkaline magmas. White (1966) believed that the wehrlite and gabbro nodules in Hawaiian alkali olivine basalt had a cumulative origin. His evidence was the apparent equilibrium of nodule with host, grain size layering and occasional poikilitic texture. Aoki (1968) suggested that the low calcium and sodium content of pyroxenes from wehrlite and gabbro inclusions in the Iki Island alkali basalt indicate formation at less than 35 kilometers. That fact, plus the similarity of nodule minerals to those of the host, led him to suggest a cumulate origin for the nodules.

After an extensive study of phase equilibria, O'Hara and Yoder (1967) proposed that partial melting of a garnet peridotite mantle could produce hypersthene-normative picrite basalt which would fractionate eclogite cumulates at high pressure to produce

kimberlite magma, while low pressure crystallization would produce olivine assemblages and silica-saturated tholeiite liquids. Allsopp et al (1969) presented essentially the same picture, but suggested further that the eclogite so formed may be remelted to form abyssal tholeiites and secondary eclogite slightly enriched in CaO and Al_2O_3. Sr isotope data were presented in support of their conclusions. Rickwood et al (1968) developed a model which differs from that of Allsopp et al in that the remelted eclogites produced a series of kimberlitic fluids, each of which precipitates an eclogite enriched in calcium and iron relative to its parent. Their evidence is the apparent grouping of eclogite garnet compositions into four different compositional ranges (Fig. 12, this report).

Finally, Ito and Kennedy (1968) proposed a model in which fractional crystallization of parental magma at depths of 60-70 kilometers produce alkali basalts, while crystallization from the same melt compositions at depths below 100 kilometers produce kimberlite magmas. In each case, crystal accumulates go through a sequence of olivine-rich, then pyroxene-rich, and finally garnet-rich compositions.

METHOD OF STUDY

Six inclusions were chosen from the Stockdale kimberlite for detailed study. Because Rb-Sr data comprise part of this study, three of the inclusions are xenoliths from the Precambrian basement complex. They were included in order to provide data on

the chronology of disturbances in the Precambrian, for which reason discussion of their petrology will be rather brief. The three other inclusions are basic and ultrabasic nodules of uncertain origin. Interpretation of their chemistry and petrology will comprise the bulk of this study.

The inclusions are listed below:

1139h hypersthen gabbro	
1139i diorite	basement xenoliths
1139j hypersthene gabbro	
1128d spinel-garnet metagabbro	
1128g eclogite	nodules
1141a garnet metagabbro	

Analytical Procedures

Initial mineral separation was done with a Frantz Isodynamic Separator. Bromoform and methylene iodide were then used for purification. Better than 98 percent purity was achieved for all minerals used for chemical or Rb-Sr analysis.

Thin-section modal analyses were carried out by standard techniques (Chayes, 1956). Between 500 and 1200 counts were made per sample depending on section size. Optic angles and extinction angles were determined with a four-axis universal stage. Wherever possible, optic angles were measured by direct rotation on suitably oriented grains. The majority of cases required plotting

of optic directions on a stereo net. For orthopyroxene, some values were determined by doubling the angle between the c-axis, i.e. line of intersection of cleavage planes, and one optic axis. All measurements were corrected for tilt of the stage using Emmon's (1943) chart.

Birefringence was measured with a Berek Compensator. None of the samples contains free quartz, but most do contain orthopyroxene which can also be used to obtain section thicknesses. This procedure involves first determining the optic angle of the orthopyroxene with the universal stage, followed by birefringence determination using Hess' (1960) chart of the optical properties of orthopyroxene. The thickness of the inclined section is determined after measuring retardation with the Compensator. The true angle of inclination of the section is determined on a stereographic plot and section thickness calculated from the relation:

$$\text{true thickness} = \text{thickness of inclined section} \times \cos \text{angle of inclination}$$

A possible source of error in the above procedure is the presence of aluminum and calcium in the metamorphic orthopyroxenes, although comparison of refractive indices and optic angles with the values predicted from Hess' chart suggest that the error is probably small.

Refractive index measurements were made on gelatin mounts (Olcott, 1960) using uncalibrated oils. When grain-oil indices were matched, a small amount of the oil was placed on an Abbe

refractometer and its index measured. Most of the minerals studied had a sufficiently high dispersion such that white light could be used. Plagioclase indices were measured using a sodium vapor lamp.

Most of the x-ray work was done with a Straumanis camera of 114.6 mm circumference manufactured by Philips Electronics, Inc. Molybdenum-filtered iron radiation was used with exposure times of 12 to 16 hours. Film shrinkage corrections were applied in determining d values. Gum tragacanth sample mounts were prepared using roughly the method outlined by Azaroff and Buerger (1958). X-ray data for garnet are presented in Appendix B.

Evaluation of plagioclase structural state was done with a Philips diffractometer through the parameter $\Gamma = 2\theta(131) + 2\theta(22) - 4\theta(131)$. An independent method of finding the plagioclase composition is necessary: in the present case N on (001) cleavage fragments was measured by immersion procedure. While this index does vary slightly with structural state for some compositional ranges it is virtually fixed for the compositions encountered in this study. In any event, once approximate composition is obtained, the x-ray data indicate which determinative curve shoud be used.

Chemical compositions were determined by atomic absorption spectroscopy, flame photometry, and estimation by subtraction. Al_2O_3 and TiO_2 concentrations were obtained from a Jarrell-Ash Model JA 82-518 unit using a nitrous-oxide - acetylene flame. Standards for these elements were prepared by Mr. O. K. Galle of

the Kansas Geological Survey. CaO, MgO, FeO (as total iron), and MnO were determined on a Perkin-Elmer Model 303 unit operating on an air - acetylene flame. Standards for the four elements were prepared from solutions of United States Geological Survey Rock Standards W-1 (basalt) and GSP-1 (granodiorite) prepared in the same manner as the unknowns. This procedure has the advantage that weight percent of oxide may be read directly from the working curve. Dissolution procedure involved digestion of 0.2 grams of sample in HF, evaporation to dryness, re-solution in 10 milliliters of 6N HCL, and dilution to 200 milliliters with deionized water. Aliquots of the 200 milliliter solution were then diluted by successive factors of two to obtain concentrations within the operating range of the instrument. The approximate silica percentage was obtained by subtraction. Water content was considered to be trivial and not considered.

While the last two factors introduce a systematic error, they do not affect the critical FeO:MgO:CaO ratios. The data for major oxides are presented in Tables 1 and 2. Judging from the working curves (Appendix C), accuracy for most of the oxides should be better than about $\pm$ 3 percent, while MgO should be accurate to about $\pm$ 5 percent.

Anomalously low calcium readings were obtained from the GSP-1 standard solutions, about an order of magnitude less than would be expected when compared with the W-1 solutions. Comparison of iron readings from the same solutions indicate no error in preparation. In addition, aliquots of W-1 and GSP-1 were prepared from

two separate dissolutions of each standard, and identical results were obtained in each case. Chemical interferences in the determination of calcium by atomic absorption are most commonly due to the presence of aluminum and silicon (Slavin, 1968), which are present in comparable amounts in W-1 and GSP-1. Potassium is much more abundant in GSP-1 than in W-1, however, and this element apparently has, on some occasions, interfered with calcium determinations (Slavin, 1968, Angino and Billings, 1967), although on a much smaller scale than the difficulty encountered in the present study. The problem is still unresolved. GSP-1 solutions were not employed in calcium analyses; instead, working curves were drawn from successive dilutions of the W-1 stock solution. The data thus obtained are believed fairly accurate inasmuch as the calcium concentrations appear reasonable. Since W-1 is close in bulk chemical composition to the unknown solutions, it is probable that matrix effects are largely cancelled.

Ferrous iron was determined by the standard titrimetric method using dichromate solution with diphenylamine sulfonate as the indicator (Shapiro and Brannock, 1956). Ferric iron was found by subtracting ferrous from total iron.

PETROGRAPHY

Garnet-Spinel Granulite (1128d)

This sample is a garnet-spinel pyroxenite granulite, containing clinopyroxene: 52%, orthopyroxene: 30%, plagioclase: 30%, spinel: 4%, kyanite: 4%, garnet: 2%. Sapphirine is in very minor amounts, much less that 1%. The general physical aspect of this sample is very similar to that of sample 1141a. The texture is hypidiomorphic, with interlocking subhedral grains of clino- and orthopyroxene (up to about 8mm maximum dimension) and irregular pods of plagioclase (up to about 12mm maximum dimension). Orthopyroxene is present as distinct grains, rather than as late stage rims on clinopyroxene.

The clinopyroxene (2V av. 61.5°, N = 1.696, Y:Z = 43°) is virtually identical to that of 1141a, the only difference being the absence of pleochroism. A few grains show zoning with small (ca. 2°) variations in optic angle. Black, granular material is in all grains, generally following irregular cracks although it also occurs along cleavages. In some cases this material forms a nearly complete band encircling the center of a clinopyroxene grain, suggesting that it may be related to exsolution.

Exsolution lamellae of what is apparently orthopyroxene are developed parallel to the clinopyroxene (100). They are narrower than the equivalent lamellae of 1141a - too thin for optical study. Pleochroism is absent and their relief against the

host mineral is very low. Most lamellae are terminated within their host grains. Whereas the lamellae of 1141a show straight borders, those in 1128d are distinctly crenulated. It is inferred that the higher magnesian content of parent clinopyroxene (Table 1) has limited lamellae exsolution relative to that of 1141a. There are no inclusions within the lamellae.

Orthopyroxene is present as subhedral grains comparable in size to the clinopyroxene. Crushed fragments are black, grains in thin section are pleochroic from light reddish-brown to pale green. The optic angle is 78° (-) corresponding to the composition EN 81.

Exsolution lamellae of clinopyroxene are developed parallel to the bronzite (100) (Fig. 2). They take the form of irregular wavy striae less than .005 mm in thickness which terminate within the host. Ends of the lamellae are generally thicker than the middles, sometimes by as much as .01 mm. A distinct herringbone pattern is along the lamella - host interface, and may represent a pyroxene intermediate in calcium content exsolved from the clinopyroxene.

Extinction is generally zonal. Universal stage measurements failed to reveal any differences in optic angle between zones and there is evidentally no compositional variation within individual grains. The extinction angle and herringbone structure may both be related to solid state strain.

The orthopyroxenes of 1128d are virtually identical to Hess' (1960) "orthopyroxene of the Stillwater variety", found in the

Stillwater layered intrusion.

Plagioclase has the composition An 58-61. Twinning is on the albite and pericline laws. Zonal extinction is common, and individual grains may show compositional variations of ± 3 percent An. There is no evidence of unmixing and the only inclusions are strings of bubbles. Contacts with pyroxenes are generally ragged and are often lined with garnet or kyanite, from which a reaction relationship with the pyroxene is inferred. The structural state is that of disordered (high temperature) plagioclase (Fig. 3).

Garnet is found for the most part in association with kyanite and it is apparent that the two minerals were formed during the same reaction. Well terminated garnet crystals are within plagioclase, but most of the garnet is in irregular, sometimes sinuous patches inside or along the outside edges of orthopyroxene grains. The kyanite-garnet symplectites occur where there is plagioclase. Garnet occurring within orthopyroxene either occurs with (pleonaste) spinel or with no other secondary phase.

As will be shown in the discussion section, the garnet is evidentally of two different compositions, one of which is charateristic of the kyanite-garnet assemblage. The more common composition is shown in Fig. 11.

Kyanite forms as fibrous sheaves growing into the plagioclase from orthopyroxene. It is very close to sillimanite in appearance but the 35° extinction angle distinguishes it. X-ray powder patterns have provided proof of its composition, and have also indicated the apparent existence of a garnet phase inter-

grown within the fiber bundles. This garnet is of different composition than that represented in Fig. 11.

A dark green pleonaste spinel is frequently associated with the kyanite, along the outside rims of orthopyroxene grains. This spinel is most generally included within orthopyroxene where kyanite is not developed. It generally occurs as shapeless blebs about 0.5 mm in diameter, although a few of the larger masses show incipient crystal faces. Spinel grains are rimmed by amorphous patches of sapphirine whenever kyanite is absent. The sapphirine is pleochroic from light yellowish-green to sky blue, and has a range of optic angles of 52° to 80°. An opaque mineral is generally found as an irregular band separating the sapphirine and pleonaste. It is assumed to be magnetite, left as a residuum after magnesia and alumina were removed from the pleonaste to form the sapphirine.

EXPLANATION OF FIGURE 1

Figure showing minerals of 1128d. Dark gray areas are pleonaste spinel with minor amounts of contained light gray sapphirine. Radiating lines in 1b are kyanite.

Figure 1a

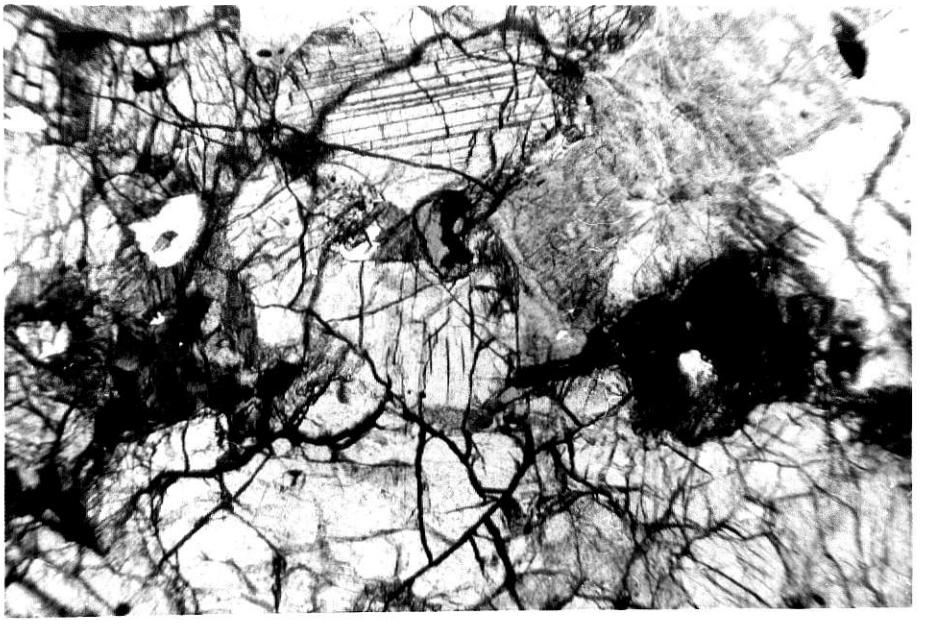

Figure 1b

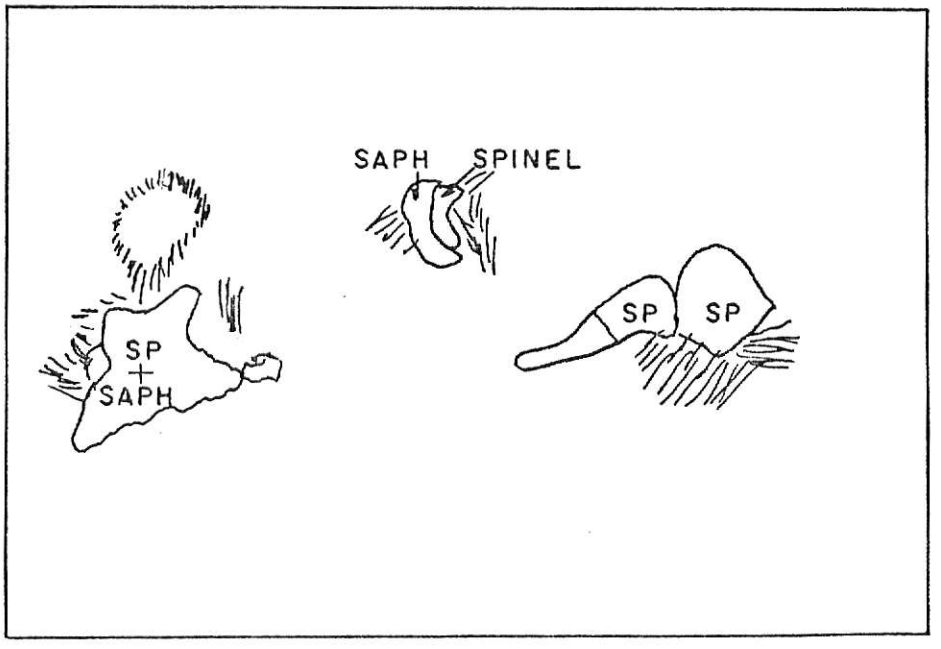

EXPLANATION OF FIGURE 2

Orthopyroxene of 1128d, showing exsolution lamellae of clinopyroxene. Other pyroxene in figure is all clinopyroxene. Figure 2a, plain light, 2b crossed polars.

Figure 2a

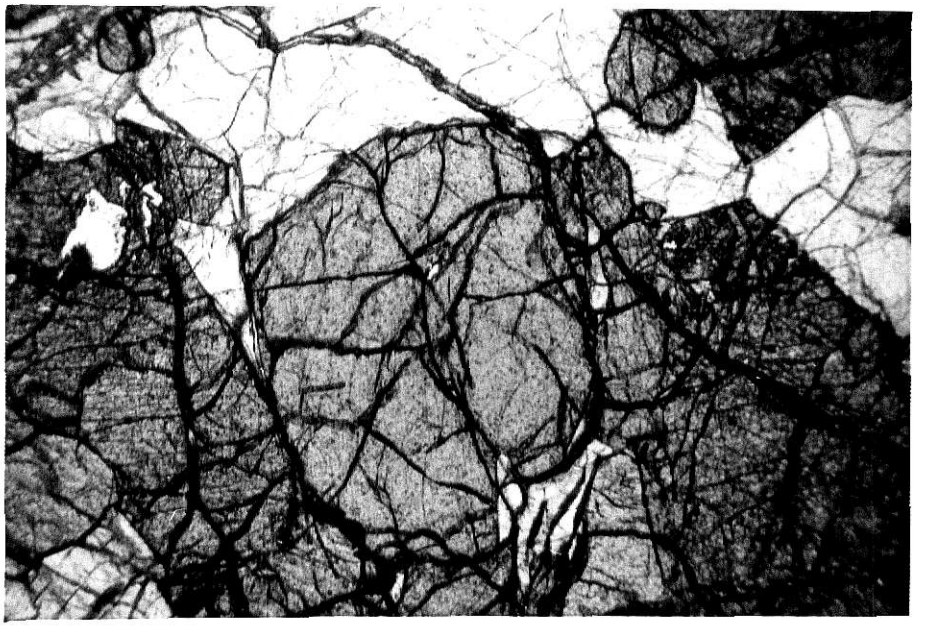

Figure 2b

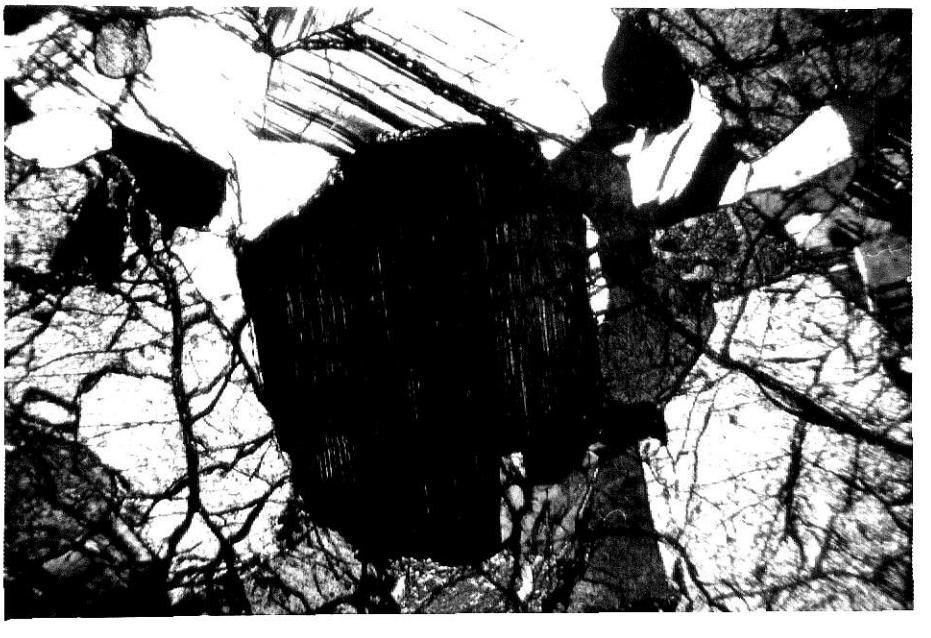

EXPLANATION OF FIGURE 3

Diagram showing structural state of plagioclase from five nodules in Stockdale kimberlite. See text for number references. $\Gamma = 2\theta(131) + 2\theta(220) - 4\theta(131)$. Diagram after Smith and Gay (1956).

Figure 3

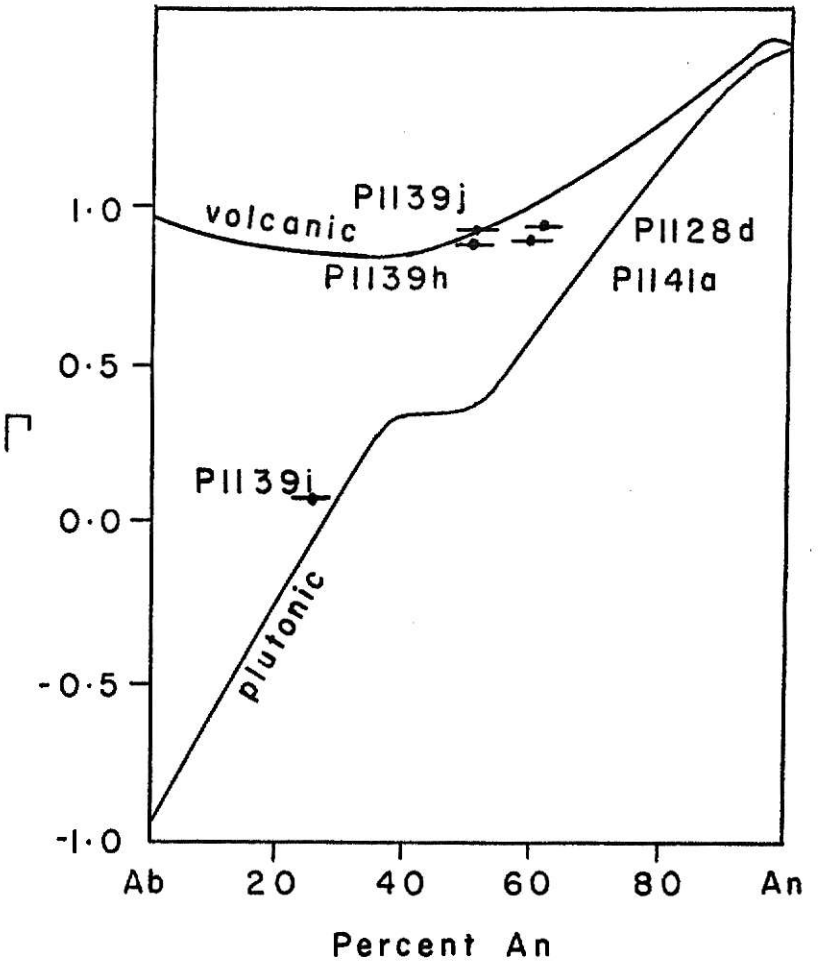
1·0
0·5
0·0
-0·5
-1·0
Γ
volcanic
P1139j
P1139h
P1128d
P1141a
P1139i
plutonic
Ab
20
40
60
80
An
Percent An

Garnet Granulite (1141a)

This sample is a uralitized gabbro or plagioclase bearing pyroxenite granulite, containing clinopyroxene: 55%, plagioclase: 21%, hypersthene: 16%, garnet: 8%. The texture is hypidiomorphic granular with large (up to 10 mm maximum dimension) interlocking crystals of pyroxene surrounding irregular pods of plagioclase. Hypersthene forms irregular patches mantling clinopyroxene. Garnet is plentiful as an alteration product and generally occurs as patches along pyroxene - plagioclase interfaces, although it also forms as subhedral and euhedral crystals approximately 0.3 mm in size. This latter occurrence may be indicative of a primary origin. A number of isometric euhedra have an apparent spinel morphology but are identical in all other aspects of appearance to the garnet. They always occur in association with the latter mineral and the proof of their being spinel is problematical.

The clinopyroxene (2V av. 61°, N = 1.702, Y:Z = 43°) is light apple green in crushed fragments and colorless in thin section, where it shows purplish-brown pleochroism. the composition from optics is approximately $Wo_{44}En_{30}Fs_{26}$, but this value is in error due to aluminum and other cations which affect the optical properties as well as stoichiometry. Composition will be treated in the discussion section.

Some clinopyroxene grains show zoning, with variations in optic angle of up to $\pm$ 4°. Cleavage parallel to (110) is well developed, as is (001) parting. Irregular curved fractures are

common, generally containing unidentifiable black granular material which may be magnetite or incipient garnet. Occasional flakes of ilmenite or rutile occur oriented parallel to (010). Small patches of secondary orthopyroxene, generally crowded with what appears to be hematite, frequently appear within individual grains.

Exsolution lamellae averaging .02 mm in width are prominently developed parallel to the host (100). These are not generally terminated within the crystal and in some cases have been further exsolved as alteration garnet. Universal stage measurements show the lamellae to consist of bronzite. 2V determinations on several grains gave consistent values of 83° (-), corresponding to the composition En 82. Lamellae show irregular, patchy extinction. Pleochroism is strong, γ bluish-green, β yellowish-brown. Black flakes which may be magnetite are regularly spaced within the lamellae, parallel to the bronzite (001). Occasional irregular patches of bronzite occur, with maximum dimensions of 0.5 mm by 0.3 mm. They are always in optical continuity with the lamellae, and may show either uniform or zone extinction. The orientation of exsolved phases is shown in Fig. 5.

Orthopyroxene occurs as either a late magmatic phase or an alteration product on clinopyroxene. It generally occurs as long, disconnected patches where clinopyroxene adjoins plagioclase. Sinuous but optically continuous patches over 4 mm long are also observed. It sometimes occurs within the clinopyroxene as small patches along magnetite-filled fracture zones. Pleochroism is

intense, α pale greenish-brown, γ dark reddish-brown. Platy inclusions of what is believed to be hematite are always present. It is possible that these inclusions account for the high Fe^{+3} content of the clinopyroxene (Table 2). In a few places, where the orthopyroxene adjoins plagioclase, a black fibrous mineral is developed. A phase of identical appearance but greater quantity is contained in sample 1128d, where x-ray powder patterns show it to be kyanite. It is presumed that the mineral in 1141a is the same.

Plagioclase (An 58) generally forms completely enclosed pods up to 6 mm maximum dimension. Each pod consists of aggregates of anhedral grains, each with rounded irregular borders. Zoning is in most, but not all grains, the range in composition being from about An 55 to An 60. Sinuous exsolution blebs of lower refractive index than the host indicate that the feldspar may be considered antiperthite.

Inclusions are ubiquitous but not abundant, consisting mainly of needles (probably rutile) and short stringers of bubbles. Twinning is generally on the pericline law. These twins frequently occur in phenocrysts showing a low degree of zoning. Albite twins are much less common. Manebach and carlsbad twinning are rarely seen. In many cases recrystallization has completely removed all twinning. Optic angle and x-ray data indicate the high temperature structural state (Fig. 3), and it is inferred that recrystallization has inverted the primary feldspar.

Garnet occurs frequently as euhedra, about 0.2 mm in diameter, along the contacts between ortho- or clinopyroxene and plagioclase. It also occurs as shapeless blebs within orthopyroxene grains and as thin shells partially mantling the orthopyroxene. Euhedra are sometimes completely surrounded by plagioclase, isolated from pyroxene grains.

EXPLANATION OF FIGURE 4

Figure showing minerals of 1141a. 4 a, plain light, 4b, crossed polars. Dark gray areas separating garnet from light colored clinopyroxene are orthopyroxene. Black areas in plain light are of ore mineral.

Figure 4a

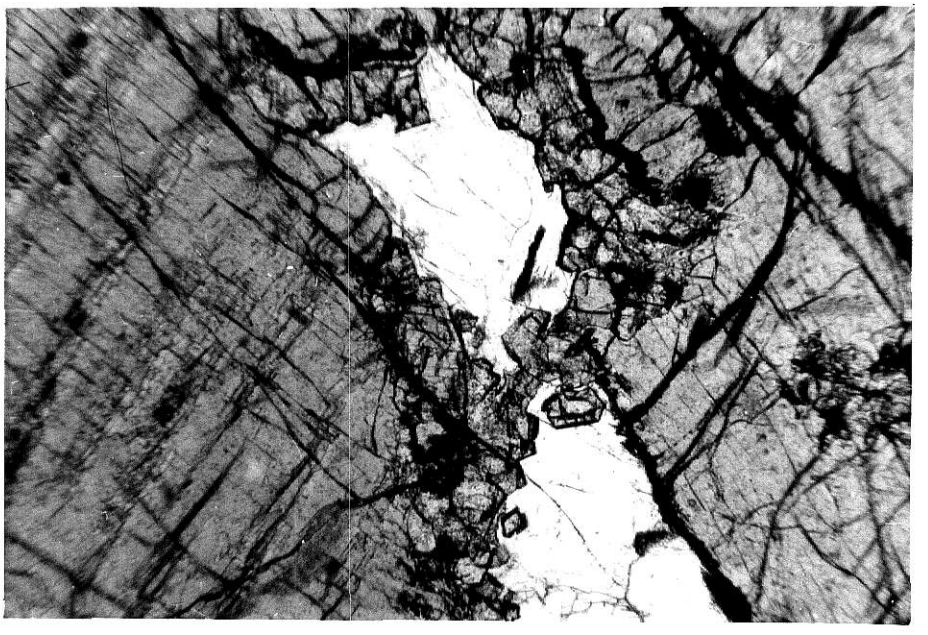

Figure 4b

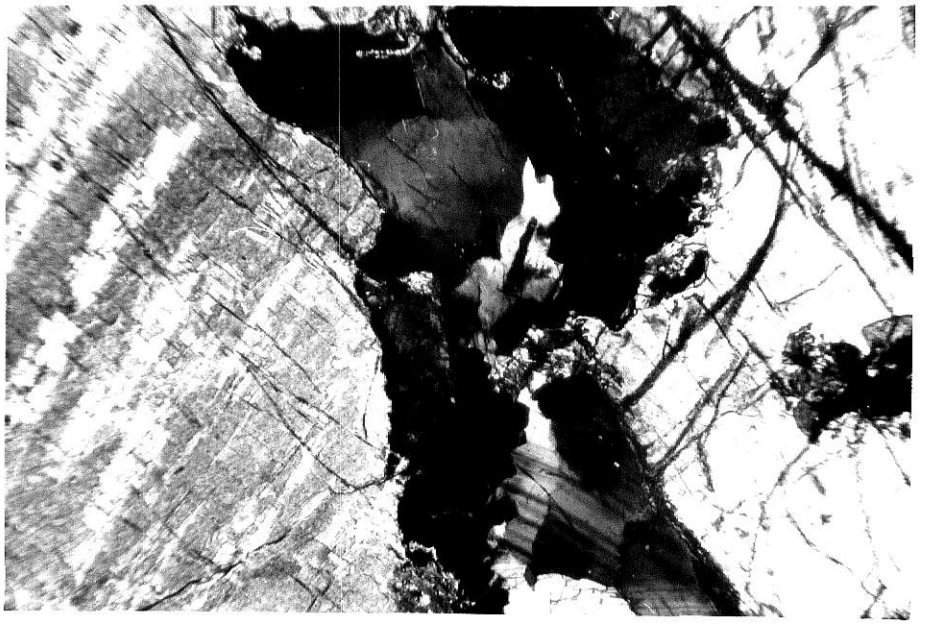

EXPLANATION OF FIGURE 5

Clinopyroxene grain from 1141a, polars crossed. Note exsolution lamellae of orthopyroxene, and flaky inclusions within the lamellae. White patches are also orthopyroxene. Irregular black patches at bottom are garnet contained within orthopyroxene. Garnet can be seen extending into the clinopyroxene along the lamellae. Also note faint herringbone pattern. Figure 5 b, optic orientation of pyroxenes shown in 5 a. Solid lines, lamellae, dotted lines, host.

Figure 5a

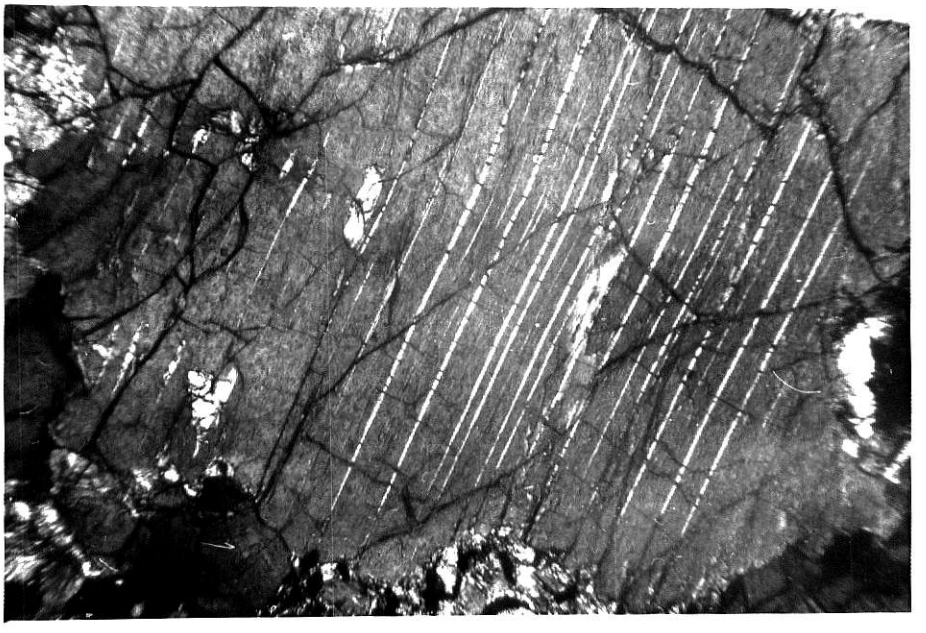

Figure 5b

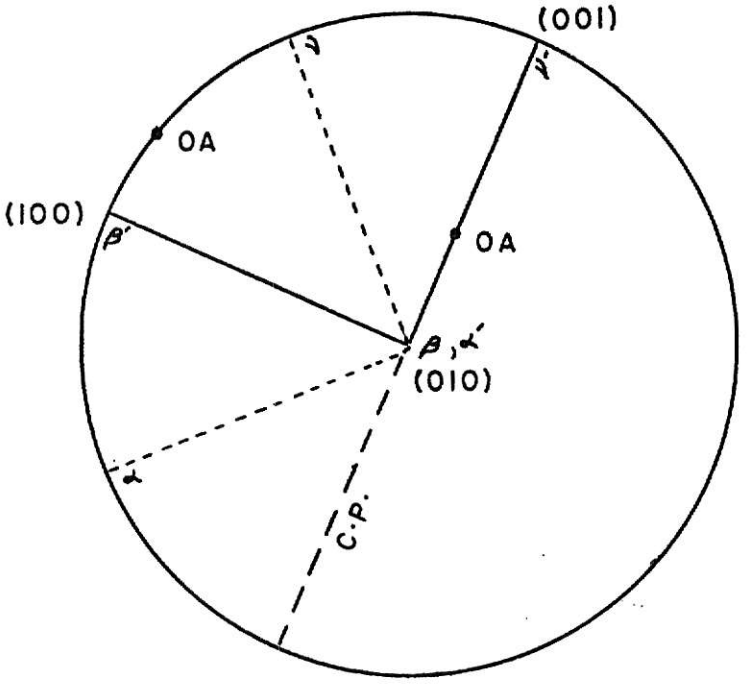

Eclogite (1128g)

This sample is an eclogite containing garnet: 87%, clinopyroxene: 13%. It consists essentially of a continuous groundmass of non-crystalline garnet in which are contained a few rounded fragments of omphacite. The pyroxene has been partly resorbed but the process was interrupted before completion.

The pyroxene is an omphacite, apple green in crushed fragments, light blue-green in thin section. Pleochroism is absent. Cleavage is frequently developed parallel to (110), but is usually absent. Parting is rarely developed parallel to (100). A few grains contain black granular material which also occurs along the borders of grains and is believed to be incipient garnet.

One pyroxene grain contains exsolution lamellae parallel to (100) that are extremely fine and have a wavy appearance, similar to typical lamellae of orthopyroxene in plutonic augites; it is assumed that they are orthopyroxene.

Garnet is massive, any crystal faces which may have been present having disappeared. In a few places granules of (presumed garnet form networks of lines which suggest the outlines of crystals (Fig. 6). For the most part, granules occur in irregular wavy lines throughout the sample. Occasional sinuous patches of a microcrystalline mineral occur within garnet. Birefringence is low, suggesting quartz (commonly found in eclogites) although a few of the patches show faint pleochroism. This mineral may be vestigal pyroxene.

A very few short stringers of dark reddish-brown mineral occur within the garnet. High birefringence suggests rutile, which frequently occurs in eclogites. The reddish-brown mineral and the mineral mentioned above each comprise less than 1 percent of the total specimen.

EXPLANATION OF FIGURE 6

Figure showing minerals of sample 1128g. 6 a, plain light, 6 b, crossed polars. Light areas in 6 b are of omphacite, black is garnet. Dark gray and black stringers in upper figure are believed to be granules of microcrystalline garnet.

Figure 6a

Figure 6b

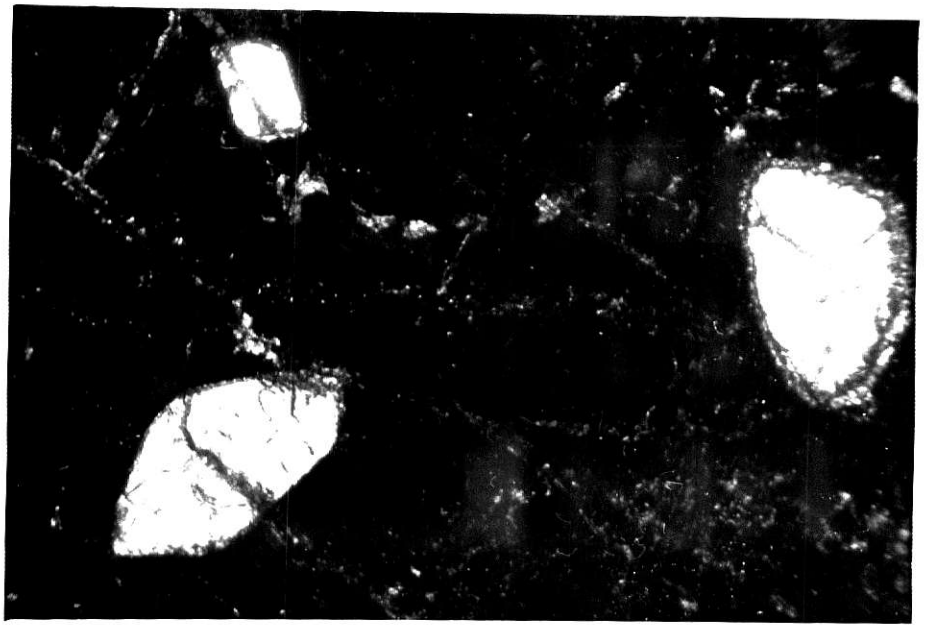

Hypersthene Gabbro (1139h)

This sample is a hypersthene gabbro, consisting of labradorite: 72%, hypersthene: 16%, augite: 11%, magnetite: 1%. this inclusion is comparable to 1139j, the main difference being in the relative amounts of constituent minerals. It possesses a hypidiomorphic-granular texture, with pyroxenes showing partial resorption. Pyroxenes average about 0.3 mm in maximum dimension. Augite has the composition $Wo_{45}En_{33}Fs_{22}$. Primary hypersthene is of the same composition as that of 1139j (En 73), but secondary hypersthene shows a range in composition of En 76 to En 83.

Plagioclase has the composition An 52, the same as in the other nodule of hypersthene gabbro (1139j). Twinning is very common, generally on the pericline law. Carlsbad, albite, and combined twins also occur. Irregular blebs of exsolved potassium feldspar are ubiquitous within the plagioclase. Extinction is oscillatory, but there is evidentally no compositional variation within grains.

EXPLANATION OF FIGURE 7

Sample 1139h. Plain light. Most of the pyroxene is hypersthene. Several grains of augite containing wavy flakes of biotite are in the top center of the photograph.

Figure 7

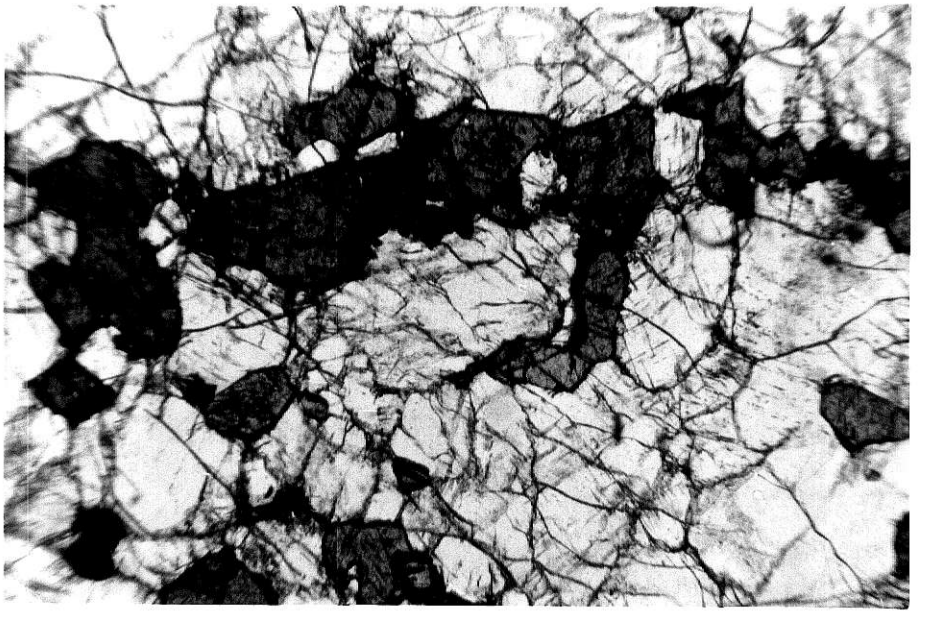

Diorite (1139i)

This specimen is a diorite, containing feldspar: 49%, hornblende: 41%, biotite: 8%, sphene: 2%. The feldspar is mainly oligoclase (An 24), but potassium feldspar is probably also present in amount less than 10 percent of total feldspar. The texture is panidiomorphic-granular, with hornblende euhedra and laths of biotite between grains of subhedral feldspar. Preferred orientation is displayed by hornblende and is especially pronounced in the biotite. Granules of sphene are ubiquitous and are generally located along the outside borders of hornblende grains from which they have exsolved.

Hydrothermal alteration has intensely affected this specimen. The outermost 5 mm has been infiltrated with veinlets of hydrothermal calcite. Within this zone hornblende is altered to ilmenite and leucoxene. Plagioclase is sericitized, and the groundmass seems to consist of serpentine and sericite. Biotite is less common than in the interior of the xenolith, but the laths which are present appear essentially unaltered. Proceeding inward, next is a zone approximately 3 mm wide in which highly altered hornblende appears. Crystals of this mineral are brown, mantled by exsolved magnetite, and have extinction angles of about 5^{o}, from which it may be assumed that they have the composition of basaltic hornblende. A few granules of sphene are present in this zone. Plagioclase is sericitized. The bulk of the xenolith is made up of the innermost alteration zone, in which green, essentially unaltered hronblende, biotite and abundant sphene appear. Plagioclase

is sericitized, but relict outlines of the feldspar phenocrysts are clearly discernible.

Completely unaltered diorite forms an oval patch about 2 cm by 0.5 near the center of the xenolith and occupying about 25 percent of the total volume of the xenolith. Feldspar in this patch frequently occurs as euhedra, generally on the order of 0.2 mm in size. About half of the feldspar phenocrysts show twinning on the albite and carlsbad laws, both types being represented almost equally. Combined twins are rare. Albite twins possess extremely wide lamellae, which is very unusual for oligoclase. X-ray data indicate that the plagioclase in this xenolith alone amongst all the inclusions studied is the low-temperature form. Potassium feldspar is virtually indistinguishable from oligoclase except for optic angle.

Unaltered hornblende forms well terminated euhedra which are very similar to the feldspar in size. Pleochroism is intense, α: light yellowish green, γ: dark bluish green. Perfect cleavage is developed in two directions at an angle of 124°. Optical properties correspond closely to values reported by Deer, Howie, and Zussman (1962) for green hornblendes from diorites. By comparison With such hornblendes, the composition is estimated to be 100: $(Mg + Fe^{+2} + Fe^{+3} + Mn) = 53\text{-}57$.

Because it is extremely pleochroic, γ dark reddish brown, α light brownish yellow, the mica has been referred to as biotite. The refractive indices of this mineral are more appropriate to the mineral phlogopite ($\beta = 1.612$). The distinction between bio-

tite and phlogopite is rather artificial however, and the mineral in 1139i is probably best described as a magnesian biotite. What is puzzling is the combination of extreme pleochroism and low indices. These two parameters generally increase together inasmuch as they are both proportional to Ti and Fe^{+3} content.

EXPLANATION OF FIGURE 8

Sample 1139i. Plain light. Hornblende clearly showing amphibole cleavage. Biotite frequently appearing dark gray because of intense pleochroism. Some laths are visible, but number is small. Sphene granules are too small to appear in photograph.

Figure 8

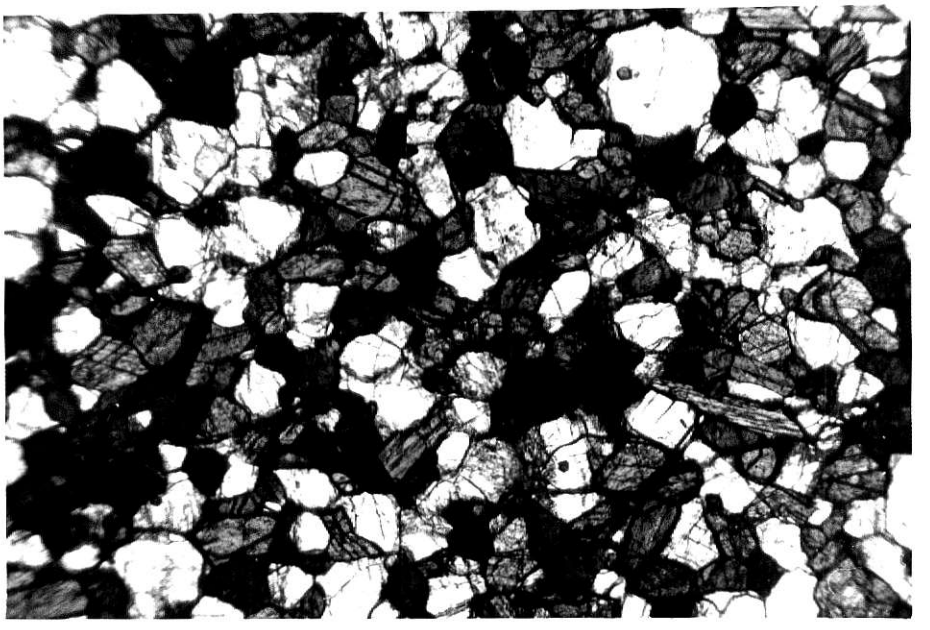

Hypersthene Gabbro (1139j)

This sample is a hypersthene gabbro, containing plagioclase: 55%, hypersthene: 25%, augite: 19%, magnetite: 1%. The texture is hypidiomorphic-granular, with well developed hypersthene euhedra, larger but generally subhedral augite grains, and anhedral plagioclase. The plagioclase forms a groundmass of large (up to 2 mm) interlocking grains, within which the pyroxene grains tend to cluster, forming a sub-glomeroporphyritic texture. The clusters are generally on the order of 2 - 3 mm in maximun dimension. Pyroxene commonly surrounds magnetite blebs, which often give the appearance of euhedra where they adjoin the straight borders of hypersthene grains. Accessory minerals are essentially lacking, although there are a few scattered granules of sphene. Feldspar grains on the outside edge of the xenolith are saussuritized, while pyroxenes are mantled with greenish brown serpentine.

The plagioclase (An 52) is generally untwinned and shows undulose extinction. Its structural state is that of the volcanic form. Because of recrystallization, there is no compositional variation across individual grains. Grains are generally on the order of 1 - 2 mm long, but there are abundant smaller (about ½ mm) unresorbed fragments of an earlier generation plagioclase. These fragments frequently show twinning, generally on the pericline law.

Irregular fractures are common, while poorly developed cleavage is less frequently observed. The plagioclase frequently contains sinuous ribbons of cryptocrystalline material which

apparently has very low birefringence. This material does not follow fractures. Its indices are lower than those of the plagioclase, and it is believed to be a mixture of cryptocrystalline feldspar (possible K-spar) and glass. Inclusions are ubiquitous, and generally take the form of rutile needles. These needles always show preferred orientation and are clearly the product of recrystallization. Vacuoles are less common.

Hypersthene ($2V = 66°$, $N\gamma = 1.706$) occurs in two habits, as primary crystallate and as alteration product on augite. The composition in both occurrences is the same En 73, suggesting that hypersthene phenocrysts were precipitating at the same time that the augite was reacting with the magma. Pleochroism (α = pale brownish red, γ = pale bluish green) is slightly more pronounced in the secondary hypersthene, and it displays much poorer crystallinity. Primary material forms phenocrysts on the order of 1 mm maximum dimension, although crystals up to about 2 mm occur. Phenocrysts are generally very well developed on all faces except (100) which is usually completely missing. Acicular inclusions are oriented parallel to (010) and in two other directions inclined $30°$ to $\underline{c}$. Platy flakes of ore mineral and biotite are often present. Cleavage is perfectly developed while parting does not generally occur.

Augite ($2V = 59.4°$, $\beta = 1.693$, $Z:\underline{c} = 37°$) generally forms subhedral phenocrysts which are conspicuously larger than hypersthene crystals. The composition from optical properties is approximately $Ca_{45}Mg_{37}Fe_{18}$, although a number of grains display concentric zon-

ing. Inclusions of biotite are always present, in some cases being confined to the center of an augite grain. In these latter cases the zoning is centered on patches of biotite, suggesting that the centers of grains are depleted in iron relative to edges. Acicular (rutile?) inclusions, oriented parallel to (100) are also common. Pleochroism is lacking. Cleavage is not generally developed.

EXPLANATION OF FIGURE 9

Sample 1139j. Large grains of augite rich in biotite inclusions. A few grains of inclusion-free hypersthene are present. Pyroxene clusters are typical of this specimen.

Figure 9

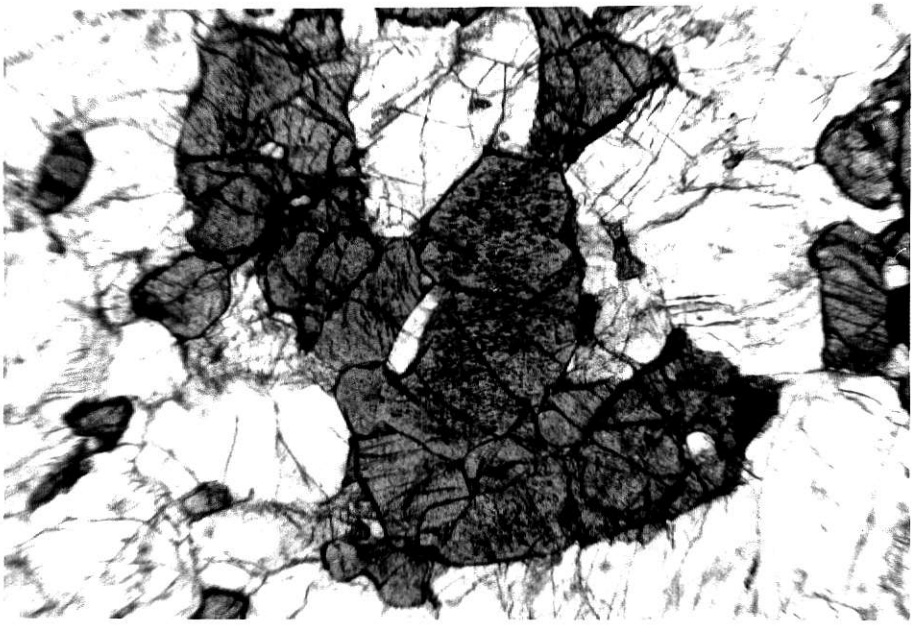

DISCUSSION

Whole-Rock Compositions

Chemical analyses of the three ultrabasic nodules and of the clinopyroxenes from two of them (granulites 1128d and 1141a) are in tables 1 and 2. CIPW norms of the three whole-rock analyses are also included. It was impossible to obtain a pure mineral separate of clinopyroxene from 1128g so that no attempt was made at an analysis of this mineral.

All three nodules correspond in bulk chemistry to undersaturated basalts. Granulite 1141a contains a small amount of normative nepheline and therefore is equivalent to an alkali olivine basalt while granulite 1128d and eclogite 1128g are chemically equivalent to olivine tholeiites. The spinel-kyanite granulite, 1128d, is less undersaturated than the eclogite, 1128g.

1141a is sufficiently close to the plane of critical undersaturation (Yoder and Tilley, 1962) that analytical error in the chemical analyses may be responsible for placing it in the alkali basalt rather than olivine tholeiite classification. The extremely high calcic values shown for the pyroxene compositions suggest that the calcium values may be too high, which would result in too low silica values since the latter are found by subtraction. This conclusion is supported because the calcic content of undersaturated basalts generally ranges around 8 to 11 percent, compared to the 14.4 percent listed for 1141a.

TABLE 1

Chemical analyses and CIPW Norms of ultrabasic nodules

	Granulite 1141a	Granulite 1128d	Eclogite 1128g
SiO_2	47.91	50.03	46.00
TiO_2	.30	.13	.58
Al_2O_3	13.13	13.98	16.43
FeO	6.12	5.88	10.16
Fe_2O_3	3.80	2.93	1.67
MnO	.13	.18	.27
MgO	11.60	13.00	14.30
CaO	14.40	12.10	8.80
Na_2O	2.50	1.48	1.60
K_2O	.11	.29	.19
	100.00	100.00	100.00
CIPW Norm			
Or		1.71	1.12
Ab	14.84	12.51	13.52
An	24.58	30.61	37.04
Ne	3.41		
Di	37.36	23.10	5.36
Hy		20.72	11.92
Ol	13.62	6.78	27.50
Mg	5.51	4.25	2.42
Il	.57		1.10
Sp		.32	
	99.89	100.00	99.98

There are certain features of 1141a which are consistent with an alkali basalt composition. One of these is the apparent secondary origin of the orthopyroxene, as opposed to the primary character of orthopyroxene from 1128d. This mineral does not belong in the mode of an alkali olivine basalt, while it is generally in basalts of tholeiitic composition. In addition, the composition of clinopyroxene in granulite 1141a is typical of that in an alkali olivine basalt: highly calcic, rich in soda, alumina, and ferric iron.

Decidedly atypical for an alkali olivine basalt is the extremely low TiO_2 content, but of probably more significance is the occurrence of exsolution lamellae of orthopyroxene. These are common in olivine tholeiites, but do not normally occur in alkali basalts (Yoder and Tilley, 1962).

The composition of eclogite nodule 1128g is compared in the following table with mean values reported for eclogite nodules of Groups 1 and 2 (see section on garnet compositions) of Rickwood et al:

	Group 1	Group 2	1128g
SiO_2	46.19	44.48	46.00
TiO_2	.83	.48	.58
Al_2O_3	10.52	14.99	16.43
Fe_2O_3	6.16	6.79	1.67
FeO	8.34	7.13	10.16
MgO	14.48	12.16	14.30
CaO	9.20	10.83	8.80
K_2O	.58	.33	.19
Na_2O	1.44	.77	1.60
	97.91	98.31	100.00

Taking the compositions of the African nodules as standards, 1128g is notably high in alumina and ferrous iron content and is extremely low in ferric iron. The latter especially surprising in that hematite occurs in 1128g, although in minor amounts. Apparently the amount of acmite molecule in the clinopyroxene is much less than typical for eclogitic pyroxene.

Composition of Pyroxene

Chemical analyses of the clinopyroxenes were recalculated on the basis of six oxygens and the data are presented in Table 2. The Z site and the X plus Y sites should each add to two. It is apparent that there is considerable error in the analyses, probably most of which is due to the calcium values, for reasons previously discussed.

Significant information is provided by the analyses in spite of the apparent errors. White (1964) has shown that clinopyroxene may be defined as granulitic or eclogitic on the basis of its tschermakite/jadeite component ratio. While White calculated the absolute weight percents of each molecule in his samples, the ratio of the two may be calculated if accurate Na_2O, Al_2O_3, and Fe_2O_3 values are available. The procedure is to assign all the Fe_2O_3 and an equal amount of Na_2O to acmite, the remaining Na_2O and an equal amount of Al_2O_3 to jadeite, and the remaining Al_2O_3 to tschermakite. Precise CaO values are not needed.

The above operation was done for the two pyroxenes studied and lines of equal tschermakite/jadeite ratio drawn on Fig. 10.

Table 2

Chemical analyses of clinopyroxenes from 1128d and 1141a

	Granulite 1128d	Granulite 1141a
SiO_2	44.67	39.97
TiO_2	.23	.33
Al_2O_3	10.11	10.77
FeO	4.20	5.12
Fe_2O_3	2.27	5.10
MnO	.12	.19
MgO	12.00	10.90
CaO	24.60	25.40
Na_2O	1.75	2.20
K_2O	.05	.02
	100.00	100.00

Numbers of ions on the basis of six oxygens

Si	1.6773	2.1245	1.5419	2.0315
Al	.4472		.4896	
Ti	.0081	1.999	.0120	2.1820
Fe^{+2}	.1320		.1653	
Fe^{+3}	.0640		.1478	
Mn	.0038		.0063	
Mg	.6717		.6268	
Ca	.9898		1.0498	
Na	.1272		.1646	
K	.0012		.0098	
	4.1190		4.2135	

EXPLANATION OF FIGURE 10

Boundary between eclogitic and granulitic pyroxenes clinopyroxenes on the basis of percent jadeite vs. percent tschermakite. Two dashed lines show values Jd/Ts for pyroxenes from nodules 1128d and 1141a. Figure after White (1964).

Figure 10

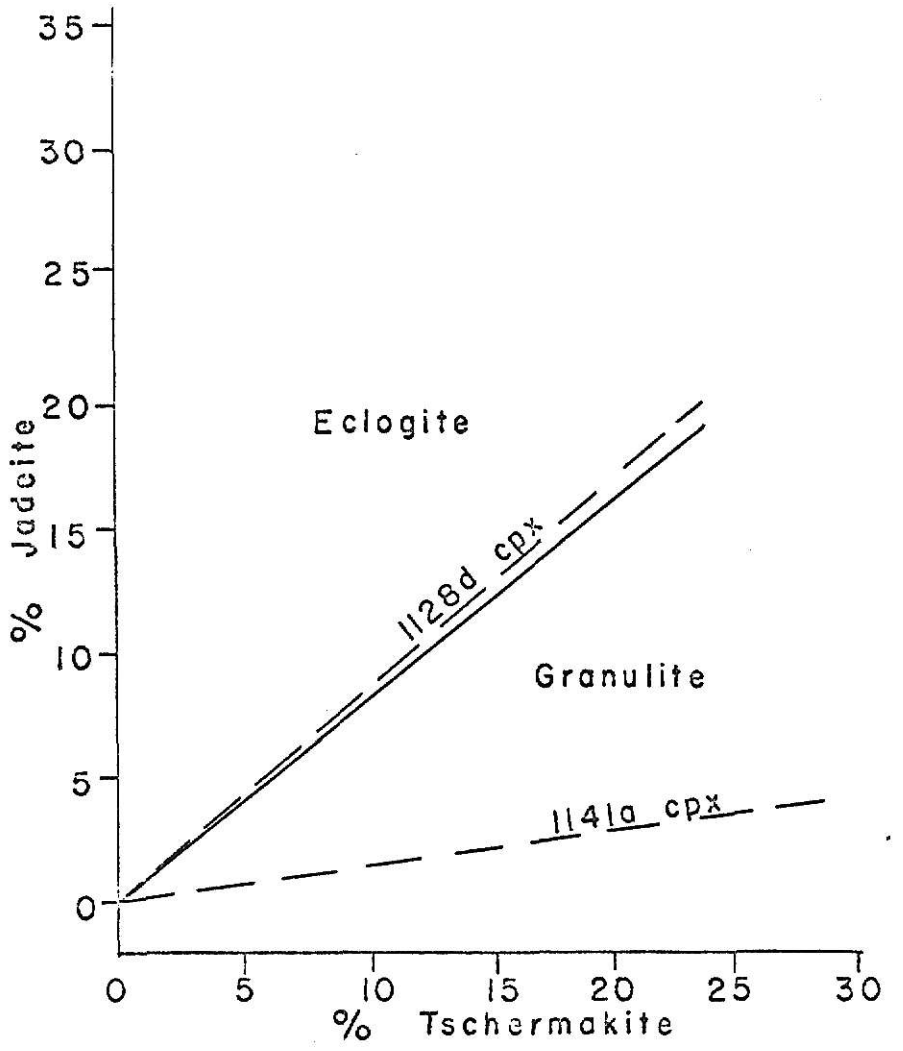
35
30
25
20
15
10
5
0
% Jadeite
Eclogite
1128d cpx
Granulite
1141a cpx
0
5
10
15
20
25
30
% Tschermakite

The facies boundary lines were taken from White's (1964) paper.

The 1141a pyroxene is clearly of granulitic composition. The pyroxene from 1128d falls almost precisely on the granulite-eclogite boundary. Inspection of Table 1 indicates that the bulk chemistry of the two pyroxenes is remarkably close. The explanation for the great difference in slope of the lines in Fig. 10 is a very high Fe_2O_3 content in 1141a which means that most of the Na_2O is taken up in the acmite molecule. The actual Na_2O content of the two pyroxenes is quite low for typical eclogitic pyroxenes, but omphacites with similar Na_2O contents are indeed known, one such being a specimen from an eclogite nodule found in the Dodoma kimberlite pipe in Tanzania (O'Hara and Yoder, 1967). The African and 1128d pyroxenes are compared in the following table:

	Dodoma	1128d
SiO_2	52.04	44.67
TiO_2	.54	.23
Al_2O_3	6.93	10.11
Fe_2O_3	2.59	2.27
FeO	4.10	4.20
MnO	.09	.12
MgO	11.65	12.00
CaO	19.49	24.60
Na_2O	2.22	1.75
	99.65	100.00

Very similar amounts of Na_2O, FeO, Fe_2O_3, and MgO are in the two pyroxenes. However, Al_2O_3 and Cao are greater in 1128d, corresponding to a greater Ca-tschermakite content and, presumably, somewhat lower metamorphic grade. The latter is also suggested by the fact that Na_2O is somewhat less in 1128d.

Kushiro (1969) has shown that, in the absence of quartz, a

continuous range of Ca-tschermakite and jadeite solid-solution is possible in diopside under P-T conditions corresponding to the eclogite facies. He does not consider the effect of hedenbergite molecule, however, which would presumably take up some of the Na_2O as acmite. Nonetheless, after comparison with the Dodoma pyroxene, it seems that the clinopyroxene from 1128d may very well belong to the eclogite facies.

Composition of Garnet

Compositions of the garnets from the three nodules were determined from refractive index and lattice constant measurements. The above two parameters were plotted on Winchell's (1958) chart, a section of which is shown in Fig. 11. The chart is ambiguous in that any particular combination of refractive index and lattice constant may correspond to two garnet compositions. Rickwood et al (1968) assumed that the composition of their garnet samples were within the range of values reported for other kimberlite nodule garnets in the literature. The same assumption is made in the present work.

The four areas in Fig. 11 outlined in solid lines correspond to compositional ranges found by Rickwood et al (1968) for garnets in 134 nodules from 17 South African kimberlite localities. The garnet from sample 1141a falls within the pyroxenite garnet field so defined, while the minerals from the eclogite, 1128g, and possible eclogite, 1128d, are contained within the compositional ranges of eclogite garnets. Note especially that the garnet from

sample 1128d (which contains kyanite) plots well within the area for South African kyanite eclogites.

Garnets from 1141a and 1128g are virtually identical in their ratio of almandine to pyrope, but garnet from 1128g is enriched somewhat in grossular component. Garnet 1128d is enriched in pyrope and grossular with respect to both of the other garnets.

Studies by Green and Ringwood (1967) indicate that pyrope content increases with pressure. Rickwood et al (1968) point out that bulk composition of the rock is of importance in determining garnet composition, but in comparing samples 1128d and 1141a it is the nodule containing the lesser amount of ferrous iron (1128d) which contains the garnet having the greater amount of pyrope component. This seems to be strong evidence that distinctly different pressures of formation are expressed by the two samples.

Different garnet-forming reactions are indicated for the two nodules. The fact that garnet 1128d plots in the field of kyanite eclogites (Fig. 11) suggests that the kyanite and garnet are involved in a reaction relationship. On the other hand, Sobolev et al (1968) demonstrated that in grospydites and kyanite eclogites with low Na_2O content, less than about 6 percent Na_2O in pyroxene, a continuous range in garnet CaO content from about 30 percent to 81 percent grossular molecule is possible. The latter implies that both garnet composition and presence or absence of kyanite may be functions of bulk composition, but need not be involved in the same reaction.

There apparently are two garnet compositions in 1128d. The usual composition is shown in Fig. 11, but a second garnet seems to be intergrown with the kyanite. The evidence is a group of four lines in the back-reflection region of x-ray powder patterns of the kyanite. The reflections cannot be identified as belonging to any other likely mineral, but seemingly can be indexed on the garnet space group. The lines and derived lattice constant from each are listed below:

d	hkl	a
.9814	(12.2.0)	11.939
.9981	(884)	11.977
1.0916	(10.4.2)	11.958
1.1073	(10.4.0)	11.926

The lines are faint and blurred, so that accurate measurement of d was very difficult, which probably accounts for the spread of a values.

The unit cell for the presumed garnet corresponds to a composition involving grossular-andradite-almandine. Almandine may or may not be present, but grossular and andradite both are included in the composition.

The garnet-forming reactions represented in sample 1128d are inferred from ambiguous textural relations and the following interpretation is considered to present only the most likely reactions. There is a considerable element of uncertainty involved.

It is believed that a two stage process occurs, in which garnet and kyanite are formed simultaneously:

(1) 3 anorthite = grossular + 2 kyanite + quartz

(2) orthopyroxene + kyanite = almandine-pyrope + quartz

Reaction (1) accounts for the Ca-rich garnet interstitial to the kyanite. Reaction (2) is inferred from the commonly observed intergrowths of kyanite and orthopyroxene bordering plagioclase grains, and has been postulated by several authors (Green and Ringwood, 1967, Green, 1967). Both reactions are simplified, in particular (2) which must account for calcium in the garnet. An alternative reaction is (Ito and Kennedy, 1968):

(3) anorthite + 2 orthopyroxene = pyrope-almandine-grossular + quartz

A number of garnet-forming reactions involving clinopyroxene are reported in the literature, but it appears that only orthopyroxene is involved in garnet development in 1128d. Free quartz is not observed in thin-section, but Ito and Kennedy (1968) pointed out that it may be in the form of interstitial glass and easily missed. A plausible reaction which would take up any free quartz is:

(4) Al-orthopyroxene + quartz = orthopyroxene + kyanite + grossular

Sample 1141a contains only one composition of garnet, which quite clearly is derived from the orthopyroxene. The apparent reaction is either (3), or the simplified reaction (Green and

Ringwood, 1967):

(5) Al-orthopyroxene = pyrope-almandine + orthopyroxene

The above reaction is suggested by the usual presence of some orthopyroxene with the garnet. While one interpretation is that the process of garnet formation was interrupted, another possibility is that all potential garnet had exsolved, leaving orthopyroxene depleted in alumina.

Conditions of Formation

Green and Ringwood (1967) showed that for rocks of basaltic composition there is a continuous transition series between assemblages classed as gabbroic (formed at less than 7 kilobars pressure) and assemblages classed as eclogitic (over 21 kilobars pressure). Mineralogical changes within the transition interval include a gradual increase in garnet and pyrope content of the garnet, and a gradual decrease in plagioclase and anorthite content of the plagioclase. It is believed that nodules 1128d and 1141a represent different P-T conditions within this transition region. Unless otherwise indicated, the following discussion is based on data by Green and Ringwood (1967).

Reaction (1) occurs at a pressure of about 23.7 kilobars at a temperature of 1000° C. Reactions (2) and (3) involve solid-solutions and are spread out over a wide P-T range.

Reaction (4) has not been found in the literature, but since it entails removal of tschermakite from an alumina-rich pyroxene,

upper granulite or eclogite facies is indicated. Reaction (5) occurs over a pressure range of 16 - 20 kilobars.

Reaction (1) seems to have occurred in 1128d from textural and x-ray studies, but it should be expected to occur only in rocks which have lost either all orthopyroxene or anorthite through a reaction such as (3). Possible explanations of this anomaly are a high albite content, which is known to extent the stability field of plagioclase, or jadeite solid-solution in the orthopyroxene. The validity of reaction (1) in the present case must be accepted with some reservations.

Since (5) is apparently the only garnet-forming reaction in sample 1141a, somewhat lower pressure conditions are suggested. The fact that some of the bronzite exsolution lamellae in the clino-pyroxene of 1141a have been garnetized suggest the additional reaction:

(6) Al-clinpyroxene + 2 hypersthene = pyrope-grossular-almandine + clinopyroxene

This reaction proceeds to the right under conditions similar to those of reaction (5).

The above discussion is highly speculative, and it would be quite surprising if the relations presented actually corresponded to reality. In addition to the compositions of the phases, another point of uncertainty is the temperature at which a proposed reaction occurred.

Fortunately, the basis for a more concrete discussion of P-T conditions is provided by sapphirine, pleonaste, and kyanite in sample 1128d. From textural relations, sapphirine appears to form by either the reaction:

(7) Al-orthopyroxene = spinel + sapphirine

or

(8) orthopyroxene + spinel + kyanite = sapphirine

According to Fig. 12, reaction (8) may be expected to proceed to the right between 7 and 14 kilobars. However, one area of the thin section shows the assemblage orthopyroxene, pleonaste, kyanite, sapphirine, and garnet, which could occur in an equilibrium assemblage only at the invariant point at 700 C°. and 13.5 kilobars. This assemblage is probably not at equilibrium, and may in fact be retrograde. Nonetheless, it is suggested that the nodule may have been subjected to P-T conditions near the invariant point. If equation (2) is valid, then a minimum pressure of 17 kilobars is indicated as pressure goes to the right of the orthopyroxene + kyanite = garnet + quartz boundary line. In any event, temperature is inferred to be close to the sapphirine boundary line because of the orthopyroxene + spinel assemblages. Boyd and Macgregor (1964) report that solid-solution of enstatite in most clinopyroxenes from kimberlite nodules indicates temperatures of about 900 - 1000° C, which is somewhat high for the present case but still quite low for magmatic conditions.

The phase diagram for the enstatite - diopside system is shown in Fig. 13 (Davis and Boyd, 1966). The phase boundaries

EXPLANATION OF FIGURE 11

Compositions of garnets from three Stockdale nodules. Six outlined areas are compositional ranges of garnets South African nodules (after Rickwood et al, 1964).

K = garnets from kyanite eclogites.

C = garnets from corundum-bearing eclogites.

Upper dashed = garnets from pyroxenite nodules

Lower dashed = garnets from peridotite nodules

Figure 11

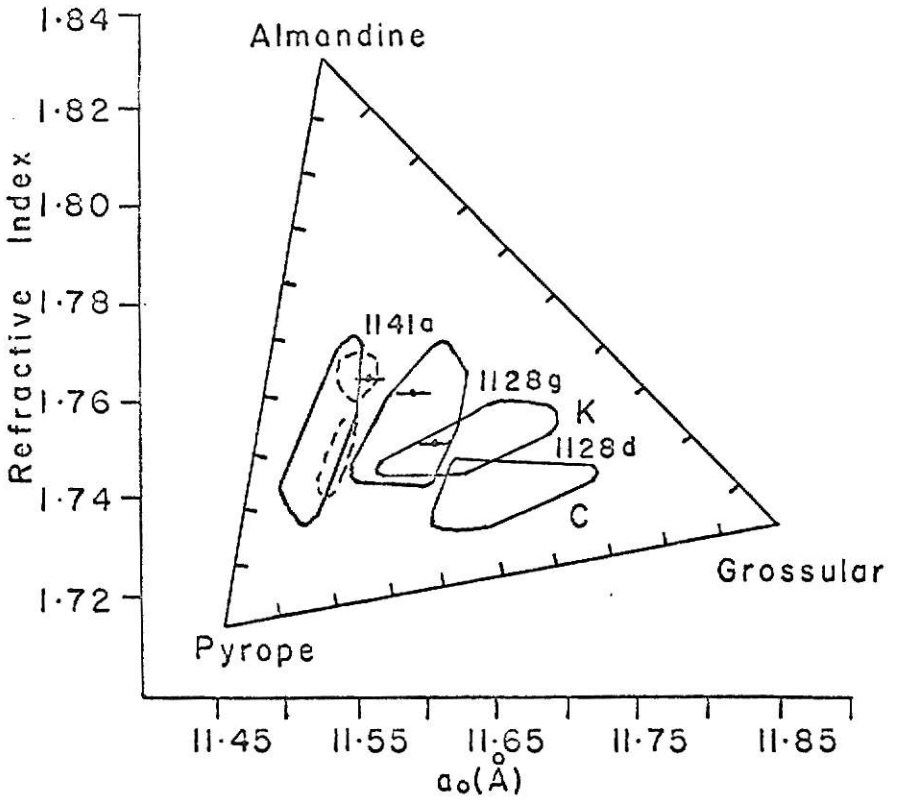
Almandine
Pyrope
Grossular
Refractive Index
1·84
1·82
1·80
1·78
1·76
1·74
1·72
1141a
1128g
K
1128d
C
11·45
11·55
11·65
11·75
11·85
a₀(Å)

EXPLANATION OF FIGURE 12

Diagram showing phase boundaries of minerals found in nodules 1128d and 1141a. After Dobretsov (1968).

Figure 12

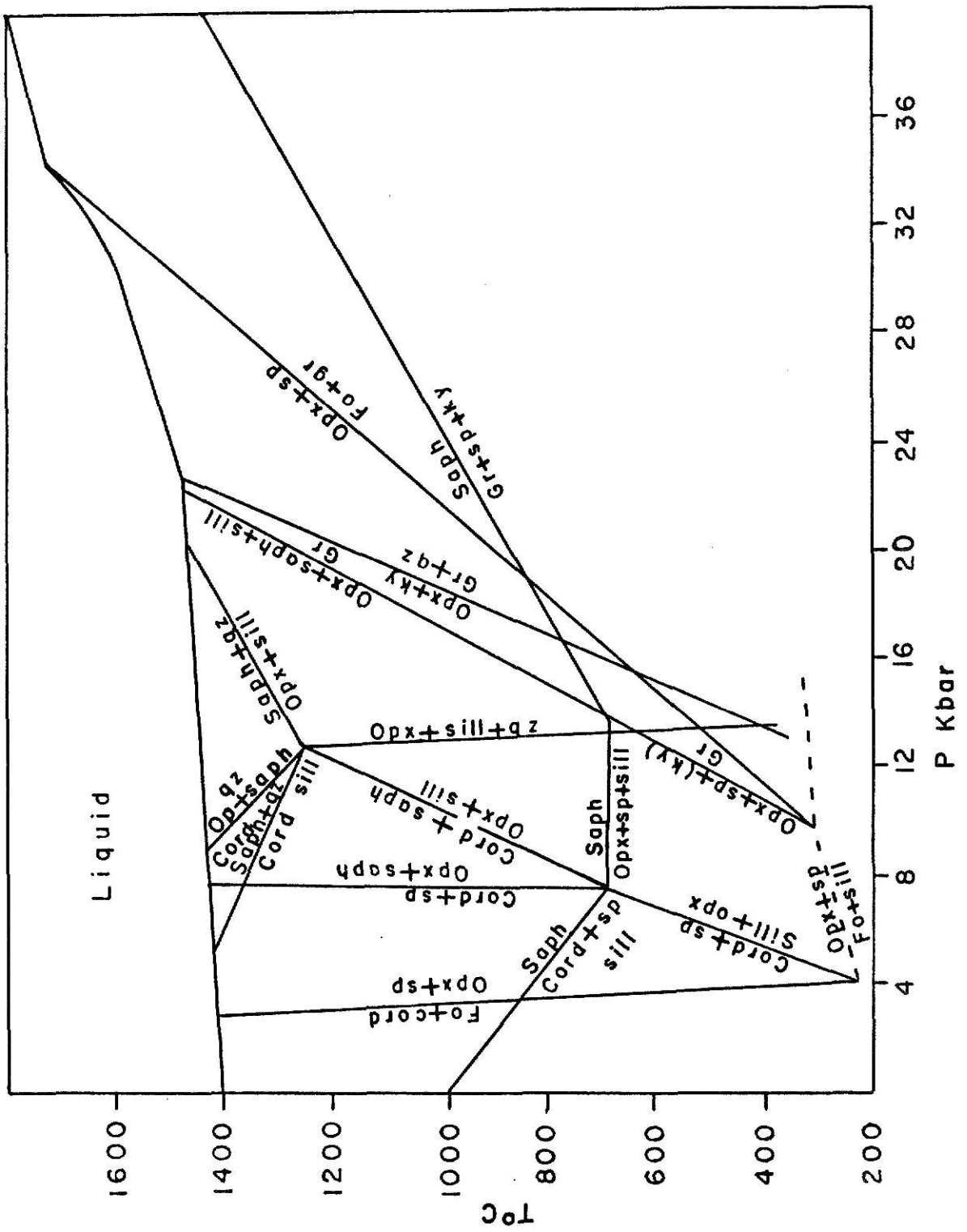
Liquid
Opx+sp
Fo+qz
Grt+sp+ky
Soph
Opx+ky
Grt+qz
Opx+soph+sill
Grt
Soph+qz
Opx+sill
Opx+sill+qz
Opx+sp+(ky)
Grt
Opx+sp+sill
Fo+sill
Opx+sp
Fo+cord
Cord+sp
Sill+opx
Saph
Cord+sp
sill
Cord+sp
Opx+saph
Saph
Opx+sp+sill
Opx+ sill
Cord + saph
Cord sill
Saph+qz
Opx+qz
qz
1600
1400
1200
1000
800
600
400
200
T°C
4
8
12
16
20
24
28
32
36
P Kbar

shown were derived at a pressure of 30 kilobars, but are essentially independent of pressure. The effect of Fe is not considered, but apparently it will cause the two-pyroxene field to contract. On the other hand, Al_2O_3 will cause it to expand, suggesting a lower equilibration temperature than the true value. It is assumed that the two effects will cancel each other to a certain extent.

Exsolution lamellae in the clinopyroxenes of both granulites suggest that the original crystallites in each case were enriched in enstatite (actually, orthopyroxene) and therefore crystallized at temperatures above 1000° C. The Ca/Mg+Fe+Ti values for the clinopyroxenes plus included exsolution lamellae of 1128d and 1141a are .99/.86 and 1.05/.94 respectively. These values are very close to almost stoichiometric clinopyroxene. From Fig. 13 it therefore follows that exsolution occurred at very low temperatures. The re-equilibration defined by the exsolution lamellae may correspond to the time of formation of the metastable five-phase assemblage mentioned earlier.

Boyd and Macgregor (1964) suggested that exsolution in slowly cooled pyroxenes occurs in two steps, with exsolution to separate grains ceasing and lamellae starting to develop at about 1000° C. It is significant that while the bulk chemistries of nodules 1141a and 1128d are similar, only 1128d contains well-developed separate crystals of orthopyroxene. It is suggested that 1141a crystallized froma more calcic melt than 1128d, so that the initial pyroxene formed as nearly pure clinopyroxene at a

EXPLANATION OF FIGURE 13

Phase diagram for the diopside - enstatite system, pressure of 30 kilobars. After Davis and Boyd, (1966). Boundary lines are affected very little by pressure.

Figure 13

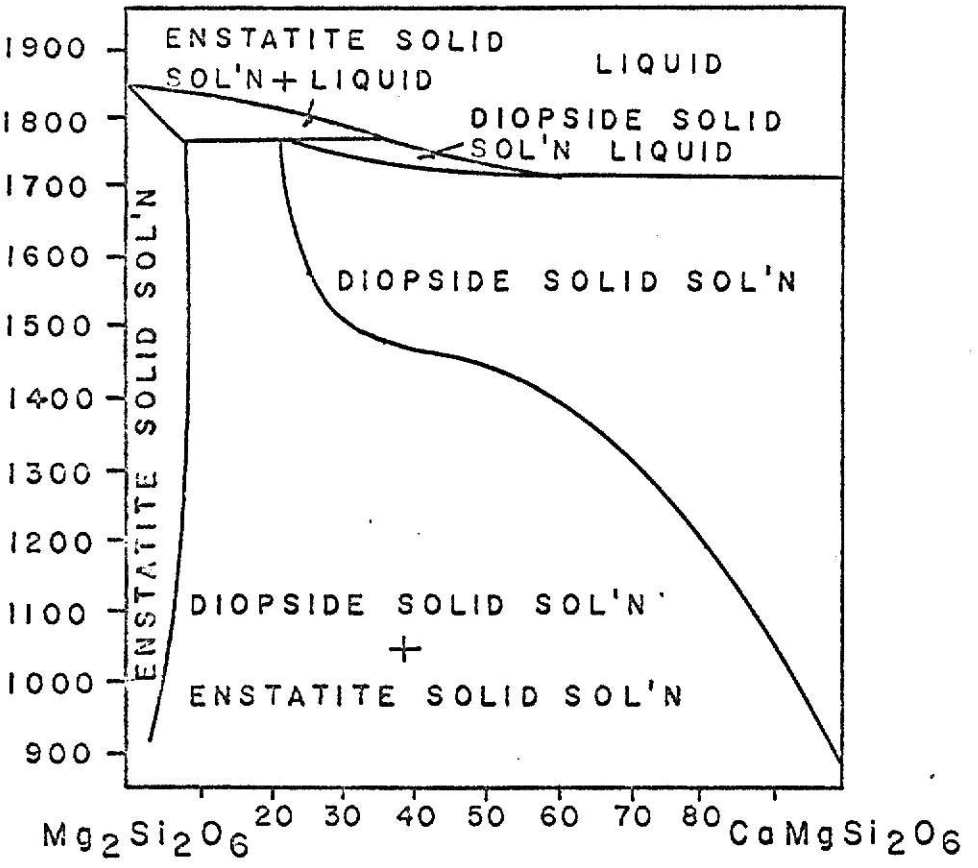
ENSTATITE SOLID SOL'N + LIQUID
LIQUID
DIOPSIDE SOLID SOL'N LIQUID
DIOPSIDE SOLID SOL'N
DIOPSIDE SOLID SOL'N
+
ENSTATITE SOLID SOL'N
ENSTATITE SOLID SOL'N
1900
1800
1700
1600
1500
1400
1300
1200
1100
1000
900
20 30 40 50 60 70 80
$Mg_2Si_2O_6$
$CaMgSi_2O_6$

temperature well below 1000°C. Examination of the bulk compositions shows that 1141a does contain over 2 percent more CaO than 1128d.

All three nodules are enriched in the "readily fusible " (Carswell and Dawson, 1970) components of Al_2O_3, CaO, Na_2O, and K_2O relative to the garnet peridotites typical of kimberlite pipes. The Fe/Mg value is similarly higher than peridotite values. These data could suggest that the nodules represent the crystallization product of the earliest liquid formed by partial melting of the mantle. Carswell and Dawson (1970) proposed that garnet pyroxenite and eclogite nodules in kimberlite represent trapped pockets of partial melt liquid, which is essentially the model proposed herewith.

Assuming a continental mantle depth of 40 kilometers (Boyd and Macgregor, 1964), the pressure at the mantle-crust boundary would be about 12 kilobars. Because the phase relations of 1128d and 1141a suggest either origin or re-equilibration at about 13.5 to 20 kilobars, an upper mantle origin is proposed. Exsolution lamellae in the pyroxene of eclogite 1128g suggest a magmatic origin for this nodule also, although presumable from deeper within the mantle than the granulites. The similarity in composition of nodules 1128d and 1141a, combined with the apparent difference in P-T conditions under which they formed, argue against crystallization from one melt. It is suggested that each nodule represents crystallization from different depths within the mantle in line with the conclusions of Carswell and Dawson.

Rb-Sr GEOCHRONOLOGY

Sample Preparation

The five nodules were studied by the rubidium-strontium geochronologic method. Isochrons were derived by computer using the procedure of York (1965). Isochrons and their corresponding ages are shown in Figures 14 and 15.

Sample aliquots for each nodule included one whole rock, one plagioclase, and one or two for pyroxene. Sample 1139i contains no pyroxene and separations of hornblende and biotite were used instead. Preparation procedure is outlined below:

1. Place powdered sample in evaporating dish and moisten with a few drops of demineralized water.
2. Add approximately three milliliters of perchloric and thirty milliliters of hydrofluoric acids.
3. Dissolve to dryness on a hot plate until white fumes are no longer given off, stirring occasionally.
4. Digest in approximately eighty milliliters of 1:1 2N hydrochloric acid. Evaporate to dryness.
5. Add ten or fifteen drops of demineralized water and let cool at least six hours.
6. Filter.
7. Add enough Sr^{85} tracer to register three times normal background.
8. Place solution on ion exchange column.

The ion-exchange resin used was Dowex 5X40. Vycor distilled 2N hydrochloric acid was used as eluant. About five or six aliquots of approximately thirty milliliters each were collected. Those with the most radioactivity and least amount of calcium

residue after evaporation were combined, the others were discarded.

Isotope ratios were determined with a Nuclide surface ionization, six inch, sixty degree direction focusing mass spectrometer. Analyses were performed by D.G. Brookins. The error about a single Sr^{87}/Sr^{86} value is $\pm$ 0.0005.

Rubidium and strontium concentrations were determined by x-ray fluorescence. U.S. Geological Survey Standard BCR-1 (basalt) was used as standard. Rb/Sr values for the unknowns were calculated either by assuming that Rb/Sr for BCR-1 equals 0.145 and correcting the ratios to this value, or by directly comparing the individual Rb and Sr peaks with those of BCR-1, and assuming that the latter contains 48.4 ppm Rb and 333.8 ppm Sr. Both methods yield results reproducible to $\pm$ 3 percent.

The data are tabulated in Table 3 and presented graphically in Figures 14 to 17. The half life for Rb^{87} was taken to be 50 b. billion years.

Discussion

The diorite (1139i) provides an age of 1,585 $\pm$ 95 m.y. with initial Sr^{87}/Sr^{86} = 0.7016 $\pm$ 0.0011. this sample has not been recrystallized and the derived age is evidentally that of formation. The low initial Sr^{87}/Sr^{86} value is consistent with a magmatic origin in the lower crust.

The norite (1139h) defines a possible isochron indicating an age of 82 $\pm$ 25 m.y. with initial Sr^{87}/Sr^{86} = 0.7062 $\pm$ 0.0002.

Brookins (1969) has provided field and isotopic evidence that the kimberlites were emplaced about 100 m.y. ago, indicating that the 82 m.y. date is probably spurious. The plagioclase structural state combined with the presence of secondary potassium feldspar indicate recrystallization under open system conditions. The apparent co-linearity of the points is probably accidental.

The norite (1139j) provides a poor 692 $\pm$ 108 m.y. isochron with initial Sr^{87}/Sr^{86} = .7051 $\pm$ 0.0007. It is thought that this date probably does indicate a real thermal event at about 700 m.y. Note that the initial Sr^{87}/Sr^{86} of both norite nodules are comparable within the limits of experimental error.

The garnet granulite (1141a) provides an isochron defining a 240 $\pm$ 8 m.y. date, with initial Sr^{87}/Sr^{86} = 0.7042 $\pm$ 0.0002. The excellent linearity of points on the isochron argues against random contamination. Lacking knowledge of the true initial Sr^{87}/Sr^{86}, however, the date can only be described as that of the last thermal event and is not necessarily the age of the rock.

The only Sr^{87}/Sr^{86} value available for the eclogite (1128g) is that of the whole-rock: 0.7044 $\pm$ 0.0005. This may serve as an upper limit for the upper mantle.

In summary, three ages of thermal events are indicated: 1,585 $\pm$ 95 m.y., 692 $\pm$ 108 m.y., and 240 $\pm$ 8 m.y. A fourth event may have occurred at 82 $\pm$ 25 m.y.

EXPLANATION OF FIGURE 14

Isochrons for hypersthene gabbro 1139j, 14a, and hypersthene gabbro 1139h, 14b. See Table 3 for analytical data.

Figure 14a

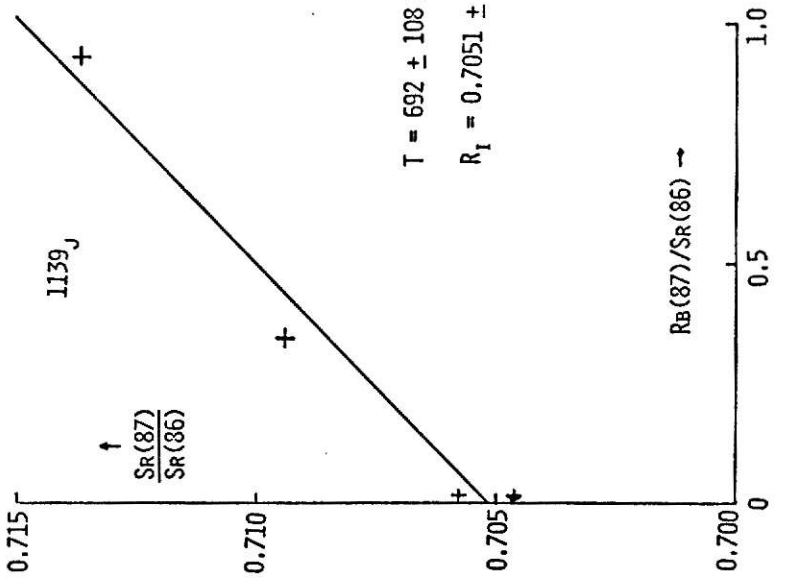

Figure 14b

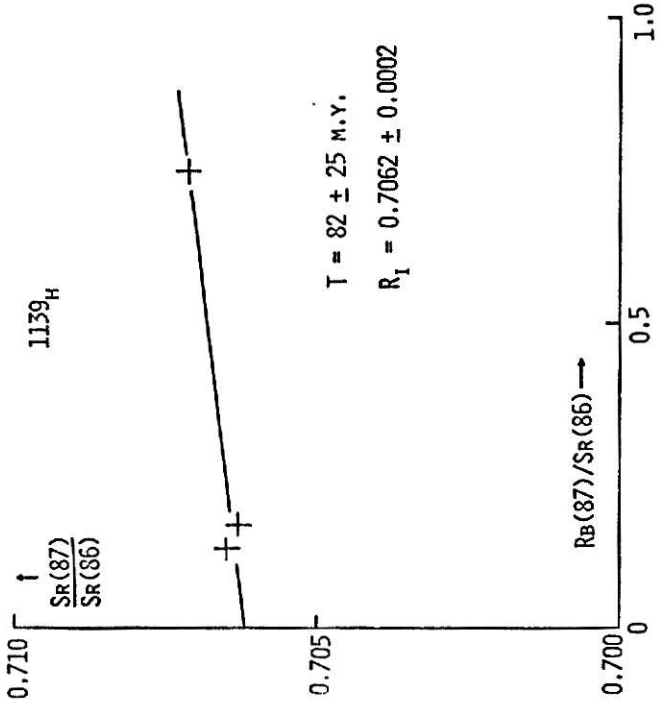

EXPLANATION OF FIGURE 15

Isochrons for garnet granulite 1141a, 15a, and diorite 1139i, 15b. See Table 3 for analytical data.

Figure 15a

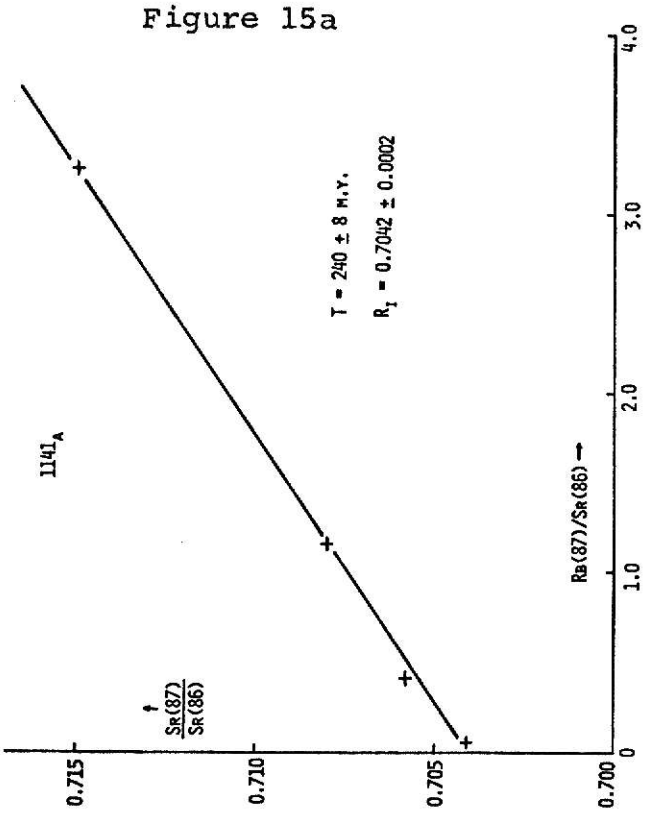

Figure 15b

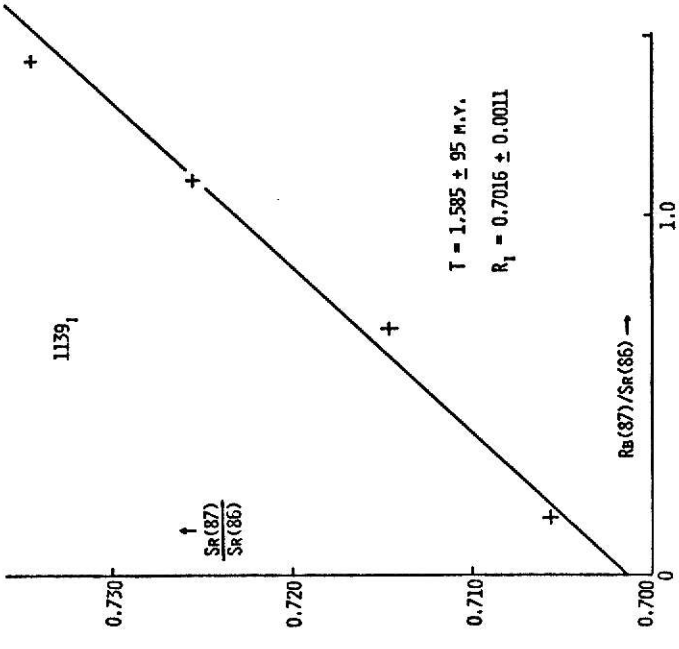

TABLE 3

Rb-Sr data

Sample	Rb (p.p.m.)	Sr (p.p.m.)	Rb^{87}/Sr^{86}	Sr^{87}/Sr^{86}
R1139h	27	462	0.17	0.7063
P1139h	49	1072	0.13	0.7065
X1139h	14	54	0.75	0.7071
R1141a	14	131	0.41	0.7058
P1141a	23	1193	0.05	0.7041
X1141a	12	30	1.16	0.7080
H1141a	20	18	3.26	0.7150
R1139i	86	358	0.70	0.7146
P1139i	80	1430	0.16	0.7056
H1139i	39	104	1.10	0.7256
B1139i	84	171	1.43	0.7345
R1139j	9	634	0.04	0.7058
P1139j	23	1416	0.04	0.7046
H1139j	10	31	0.93	0.7137
X1139j	10	78	0.34	0.7094

R = whole rock, P = plagioclase, H = orthopyroxene

X = clinopyroxene, B = biotite

SUMMARY

The inclusions of spinel-garnet metagabbro (1128d), eclogite (1128g) and garnet metagabbro (1128d) are believed to be derived from the mantle. Coexisting garnet, spinel, kyanite, sapphirine and orthopyroxene suggest minimum P-T conditions of 13.5 kilobars at 700°C for sample 1128d, while higher temperatures of formation would indicate higher pressures (Fig. 12). A pressure of 13.5 kilobars would correspond to upper mantle conditions.

Because of its lower jadeite-tschermakite ratio sample 1141a is believed to represent lower P-T conditions than the above, although it is very similar in appearance to 1128d. Presumable, uppermost mantle or possibly even lower crustal conditions are indicated.

The data on 1128g are too meager to allow any intelligent evaluation of the conditions under which it formed. Nonetheless, it is significant that while refractive index measurements show the clinopyroxene to be omphacite (Appendix A), this mineral contains exsolution lamellae of probable orthopyroxene. Such lamellae are in the clinopyroxenes of 1128d and 1141a, and are believed to be evidence for a cumulate origin for the three nodules.

The eclogitic character of the clinopyroxene and garnet of sample 1128d suggest that it is transitional in grade between 1128g and 1141a. It is doubtful that one magma chamber could

produce three nodules of such different metamorphic grade as the three under discussion, particularly in light of the similarity in bulk chemical composition of 1141a and 1128d. It is believed that the nodules formed in separate magma chambers at different depths in the mantle.

Rb-Sr data for the three crustal basement xenoliths, 1139h, 1139i, and 1139j give dates of 82 $\pm$ 25, 1585 $\pm$ 95 and 692 $\pm$ 108 million years respectively. The granulite 1141a gives a date of 240 $\pm$ 8 million years. All these data indicate the time of the last thermal event and are not the times of formation of the samples, with the exception of diorite 1139i. The high temperature structural state of the plagioclases of the two hypersthene gabbros is evidence of recrystallization.

APPENDIX A

Physical Properties of Minerals

basic granulite and eclogite nodules

1128d

clinopyroxene
2V = 60.5-62° (+)
N = 1.696
$\gamma-\alpha$ = .029

plagioclase
An 58-61
N_β = 1.562
2V = 76-77°

garnet
N = 1.751
a = 11.615 Å

orthopyroxene
En 81
N = 1.675
2V = 78 (-)
$\gamma-\alpha$ = .038

spinel
n = 1.763
a = 8.132 Å

sapphirine
2V = 52, 62
71, 80° (-)

1128g

clinopyroxene
2V = 62° (-)
N_β = 1.684

garnet
N = 1.761
a = 11.598 Å

1141a

clinopyroxene
2V = 61°
N_β = 1.702
$\gamma-\alpha$ = .029

plagioclase
An 58 av.
zoned, An
52-62
N = 1.558-
1.563

orthopyroxene
2V = 84 (-)
N = 1.712
$\gamma-\alpha$ = .012

garnet
N = 1.766
a = 11.557 Å

Physical Properties of Minerals

crustal igneous rocks

1139h

augite
2V = 60.5
N = 1.697
$\gamma : z = 44^{\circ}$
$Wo_{45}En_{33}Fs_{22}$

hypersthene

primary
2V = 66 (-)
$N\beta$ = 1.687
En = 72

secondary
2V = 74, 78
84°(-)

plagioclase
An 52
N = 1.558
$2V = 78^{\circ}$ (+)
high temp.
struc. state

1139i

hornblende
$2V = 76^{\circ}$ (-)
N = 1.672
N = 1.683
$\alpha - \gamma = .026$
$\gamma : z = 18^{\circ}$

biotite
$N\alpha$ = 1.612
$N\beta$ = 1.612

plagioclase
N = 1.545
$2V = 87^{\circ}$ (-)
An 26
low temp.
struc. state

1139j

augite
$Ca_{45}Mg_{37}Fe_{18}$

2V = 59.4°
$\gamma : z = 37^{\circ}$
N = 1.693
= 1.713

hypersthene
En 73
$N\beta$ = 1.706
$N\gamma$ = 1.715
$2V = 66^{\circ}$ (-)

plagioclase
N = 1.558
$2V = 78^{\circ}$ (+)
An 52
high temp.
struc. state

APPENDIX B

Garnet d Values

1128d			1128g			1141a		
hkl	d	I	hkl	d	I	hkl	d	I
400	2.9002	70	400	2.8952		400	2.8750	70
420	2.5988	100	420	2.5903	100	420	2.5700	100
332	2.4751	10	332	2.4683	10	332	2.4471	10
422	2.3704	15	422	2.3630	20	422	2.3484	15
510	2.2790	15	510	2.2704	20	510	2.2552	15
521	2.1212	15	521	2.1156	15	521	2.0983	15
440	2.0472	30	440	2.0451	20	440	2.0271	3
611	1.8821	40	611	1.8779	30	611	1.8677	40
444	1.6772	30	444	1.6737	20	444	1.6623	20
640	1.6132	40	640	1.6081	50	640	1.5976	50
642	1.5531	70	642	1.5492	70	642	1.5412	60
800	1.4521	5	800	1.4480	15	800	1.4443	15
840	1.2974	10	840	1.2932	20	840	1.2910	20
842	1.2678	5	842	1.2631	30	842	1.2594	30
664	1.2394	3	664	1.2327	15	664	1.2313	15
941	1.1740	3	930	1.2190	5	930	1.2175	5
666	1.0779	40	941	1.1680	12	941	1.1673	10
10 4 2	1.0604	40	862	1.1341	5	862	1.1329	5
880	1.0260	25	666	1.0774	40	666	1.0736	80
			10 4 2	1.0590	35	10 4 2	1.0558	65
			880	1.0247	20	880	1.0221	60

APPENDIX C

Working Curves for Atomic Absorption Spectroscopy

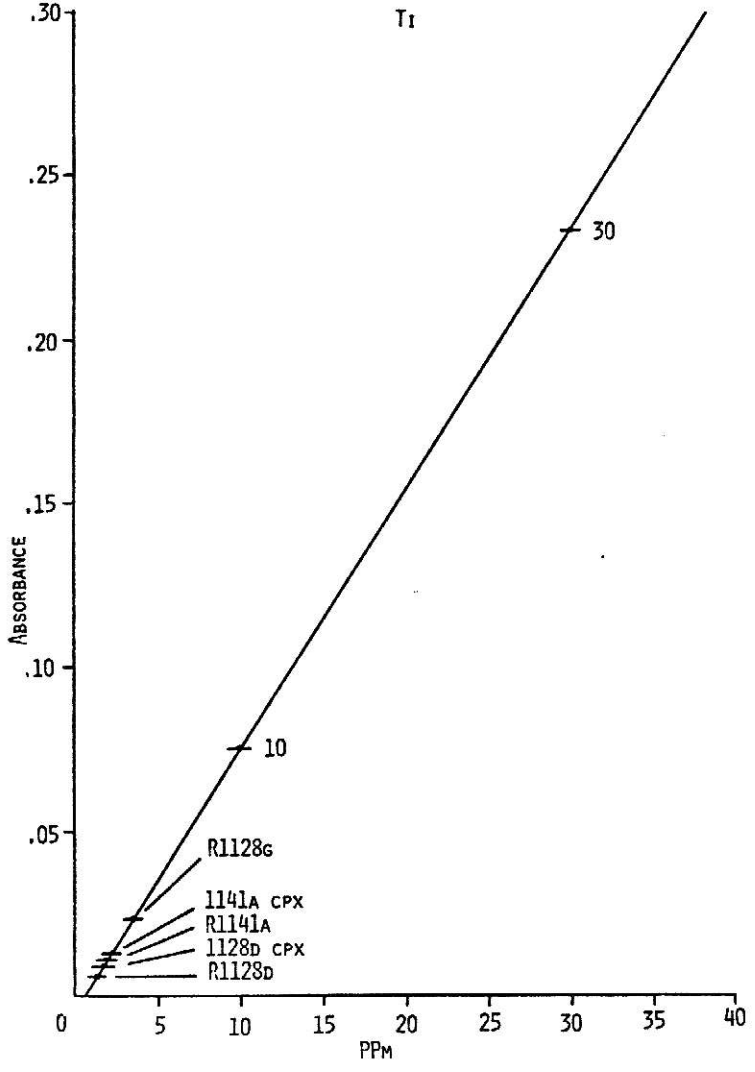
TI
ABSORBANCE
.30
.25
.20
.15
.10
.05
0
5
10
15
20
25
30
35
40
PPM
30
10
R1128G
1141A CPX
R1141A
1128D CPX
R1128D

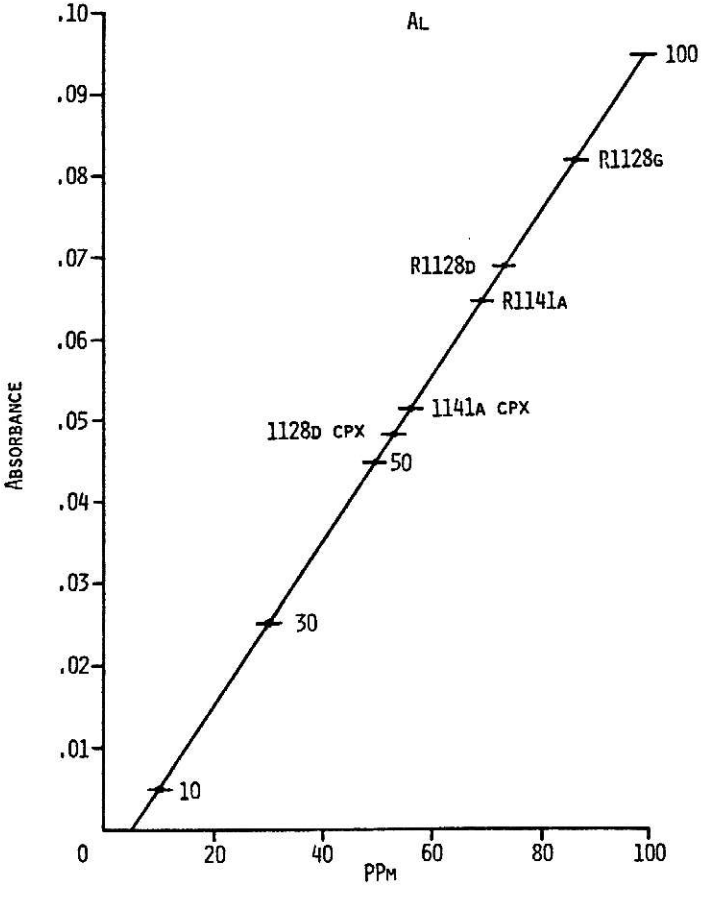
AL
ABSORBANCE
.10
.09
.08
.07
.06
.05
.04
.03
.02
.01
0
20
40
60
80
100
PPM
100
R1128G
R1128D
R1141A
1141A CPX
1128D CPX
50
30
10

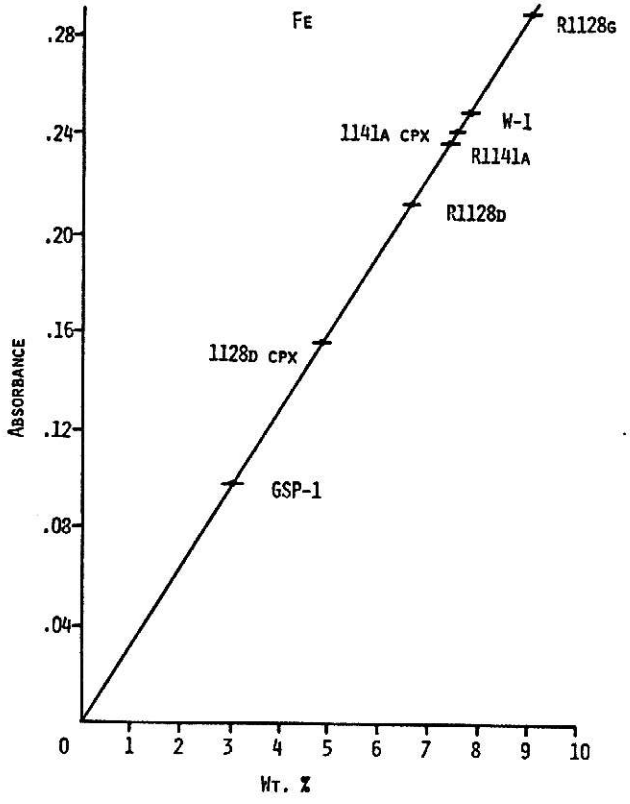
Fe
R1128G
1141A CPX
W-1
R1141A
R1128D
1128D CPX
GSP-1
ABSORBANCE
.28
.24
.20
.16
.12
.08
.04
0
1
2
3
4
5
6
7
8
9
10
Wt. %

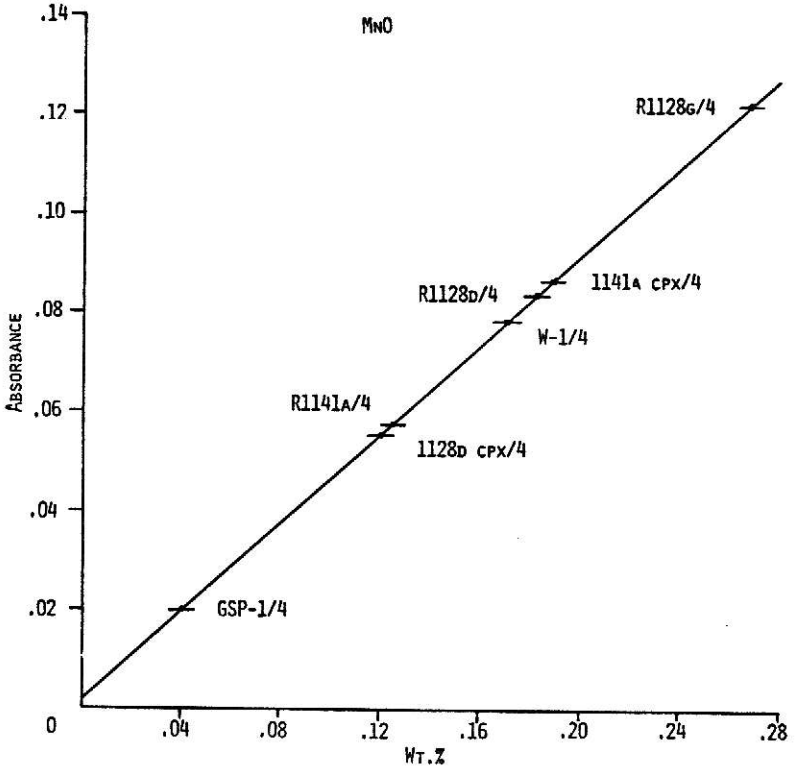
MnO
R1128G/4
R1128D/4
1141A CPX/4
W-1/4
R1141A/4
1128D CPX/4
GSP-1/4
ABSORBANCE
.14
.12
.10
.08
.06
.04
.02
0
.04
.08
.12
.16
.20
.24
.28
Wt.%

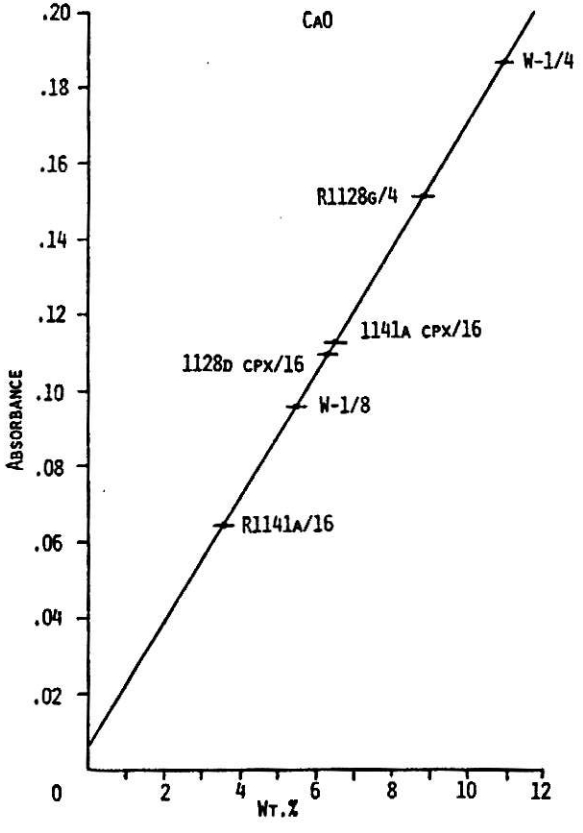
CaO
W-1/4
R1128G/4
1141A CPX/16
1128D CPX/16
W-1/8
R1141A/16
ABSORBANCE
.20
.18
.16
.14
.12
.10
.08
.06
.04
.02
0
2
4
6
8
10
12
WT.%

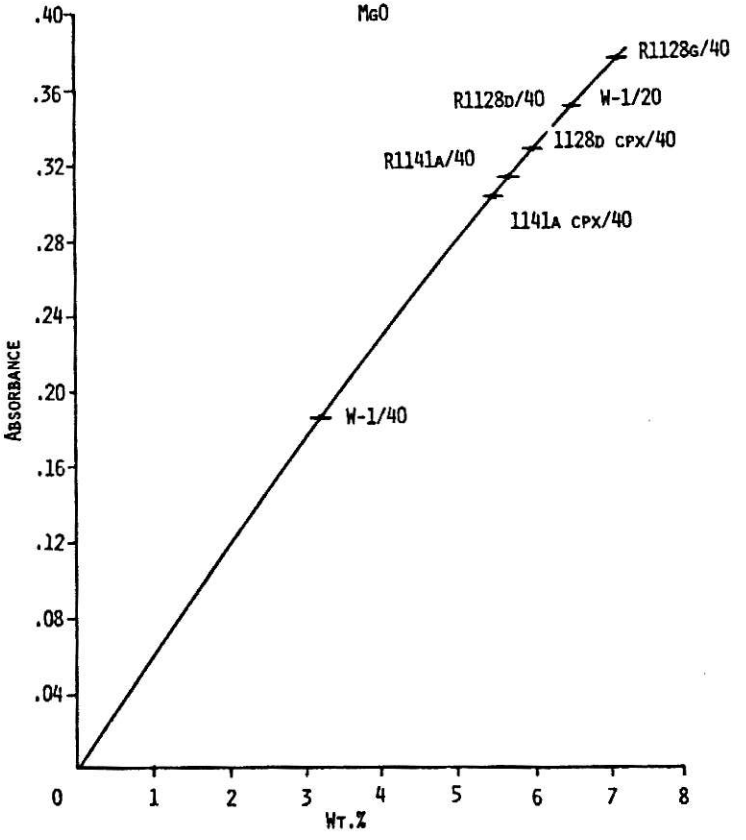
MgO
R1128G/40
R1128D/40
W-1/20
1128D CPX/40
R1141A/40
1141A CPX/40
W-1/40
ABSORBANCE
.40
.36
.32
.28
.24
.20
.16
.12
.08
.04
0
1
2
3
4
5
6
7
8
WT.%

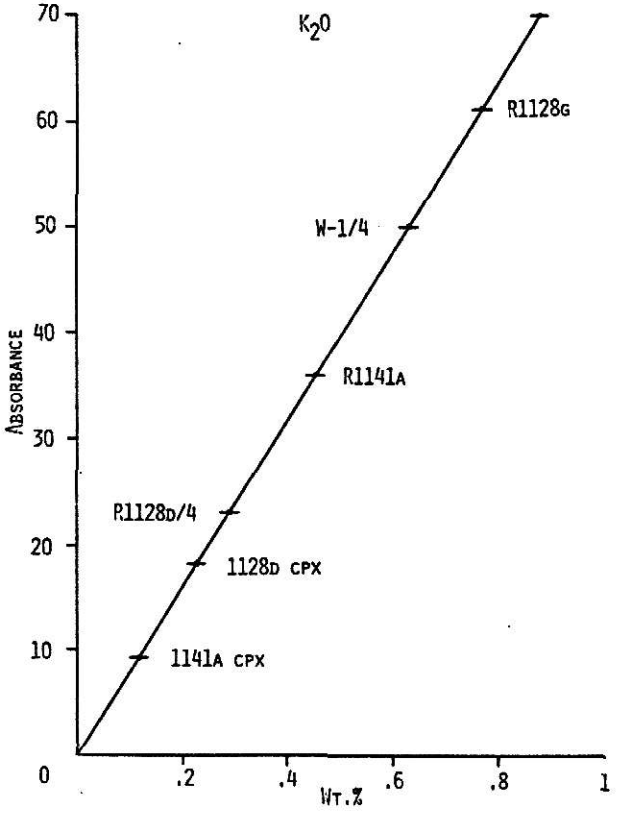
K_2O
R1128G
W-1/4
R1141A
R1128D/4
1128D CPX
1141A CPX
ABSORBANCE
WT.%
0
10
20
30
40
50
60
70
.2
.4
.6
.8
1

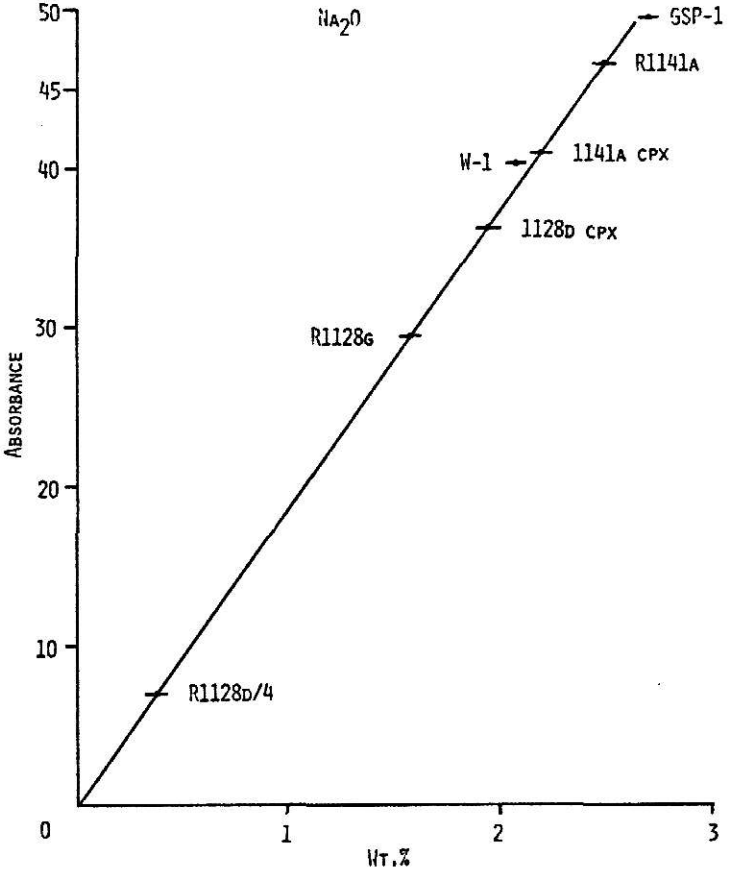
Na_2O
SSP-1
R1141A
W-1
1141A CPX
1128D CPX
R1128G
R1128D/4
ABSORBANCE
WT.%
0
10
20
30
40
45
50
1
2
3

APPENDIX D

Scandium Determination by Neutron Activation

Samples of 1128d and 1141a (granulites) and the eclogite (1128g) were analyzed for scandium content by neutron activation. This element was chosen because considerable data are available on the scandium content of basic and ultrabasic rocks (Stueber and Goles, 1967, Norman and Haskin, 1968, Taylor et al, 1969) and because the principal Sc^{46} peaks in the activation spectrum are comparatively free of interference from other elements.

Analyses were performed by irradiating samples of unknown and of pure Sc_2O_3 and comparing the Sc^{46} activity. Copper wire was irradiated at the same time as each sample and used as a monitor of neutron flux. Samples were powdered, placed in polyethylene containers, and irradiated in the Triga Mark II reactor of the Nuclear Engineering Department at Kansas State University. After irradiation gamma-ray spectra were obtained with a Technical Measurements Corporation 4096 system. A germanium-lithium detector was employed. Intensities of two scandium peaks, at 889 and 1120 kev were measured. Parts per million of scandium as calculated from the two peaks are tabulated below:

	889 kev	1120 kev	Average
1128d	51.4	-	51.4
1141a	71.6	75.3	73.5
1128g	14.2	13.8	14.0

The 1120 kev peak of sample 1128d was not measured inasmuch as it is directly on what appears to be the Compton edge of another element and hence not believed reliable.

The data for 1128d and 1141a are in good agreement with published values of Sc content of basic rocks. Stueber and Goles (1967) reported an average value for pyroxene-rich basic rocks of about 40 ppm, with maximum and minimum values of 79 and 25 ppm respectively. This is in line with the observation of Norman and Haskin (1968) that Sc generally seems to be enriched in basic rocks with high pyroxene content.

The low value obtained for eclogite 1128g is very surprising inasmuch as eclogite nodules are usually very rich in scandium. Data for a typical eclogite from Norman and Haskin (1968) indicated that most of the scandium is in the garnet phase (about 90 ppm) whereas the concentration in pyroxene is quite low (about 20 ppm). Textural evidence suggests that the garnet of 1128g was derived in the solid state from the pyroxene. The low scandium content of this nodule supports such a conclusion, and suggests further that it was formed under conditions which are not typical of eclogites in general.

REFERENCES CITED

Allsopp, H. L. and Nicolaysen, L. O., 1968, Rb/K ratios and Sr-isotopic compositions of minerals in eclogitic and peridotitic rocks: Earth and Planetary Sc. Lett., v. 5, no. 4, p. 231-244.

Angino, E. E. and Billings, G. K., 1967, Atomic absorption spectrometry in geology: Amsterdam, Elsevier, 144 p.

Aoki, K., 1968, Petrogenesis of ultrabasic and basic inclusions in alkali basalts, Iki Island, Japan: Amer. Min., v. 53 p. 241-246.

Aoki, K. and Kushiro, I., 1968, Some clinopyroxenes from ultramafic inclusions in Dreiser Weiher, Eifel: Contr. Min. Pet., v. 18, no. 4, p. 326-337.

Azaroff, L. V. and Buerger, M. J., 1958, The powder method in x-ray crystallography: New York, McGraw-Hill, 342 p.

Boyd, F. R. and Brown, G. M., 1969, Electron-probe study of pyroxene exsolution: Min. Soc. Amer. Special Publication No. 2, p. 211-216.

Boyd, F. R. and Macgregor, I. D., 1964, Ultramafic rocks: Carnegie Inst. Wash. Yearbook 63, p. 152-156.

Brookins, D. G., in press, The kimberlites of Riley County, Kansas: Kans. Geol. Surv. Bull.

Carswell, D. A. and Dawson, J. B., 1970, Garnet peridotite xenoliths in South African kimberlite pipes and their petrogenesis: Contr. Min. Pet., v. 25, no. 3, p. 163-184.

Chayes, F., 1956, Petrographic modal analysis: New York, Wiley and Sons, 113. p.

Cooper, J. A. and Green, D. H., 1969, Lead isotope measurements on lherzolite inclusions and host basanites from western Victoria, Australia: Earth and Planetary Sci. Lett., V. 6, no. 1, p. 69-76.

Davis, B. T. C., and Boyd, F. R., 1966, The join $Mg_2Si_2O_6$-$CaMgSi_2O_6$ at 30 kilobars pressure and its application to pyroxenes from kimberlites: J. Geophys. Res., v. 71., p. 3567-3576.

Deer, W. A., Howie, R. A., Zussman, J., 1963, Rock-forming minerals, v. 2: New York, John Wiley and Sons, 374 p.

Dobretsov, N. L., 1968, Paragenetic types and compositions of metamorphic pyroxenes: Jour. Pet., v. 9, no. 3, p. 358-377.

Emmons, R. C., 1943, The universal stage: Geol. Soc. Amer. Memoir 8, 205 p.

Fryklund, V. C. and Fleischer, M., 1963, The abundance of scandium in volcanic rocks, a preliminary estimate: Geochim. Cosmochim. Acta., v. 27, p. 643-664.

Green, D. H. and Ringwood, A. E., 1967, An experimental investigation of the gabbro to eclogite transformation and its petrological applications: Geochim. Cosmochim. Acta, v. 31, no. 5, p. 767-834.

Green, T. H., 1967, An experimental investigation of sub-solidus assemblages formed at high pressure in high-alumina basalt, kyanite, eclogite and grosspydite compositions: Contr. Min. Pet., v. 16, p. 84-114.

Griffin, W. L. and Rama Murthy, V., 1968, Abundances of K, Rb, Sr and Ba in some ultramafic rocks and minerals: Earth and Plan. Sci. Lett., v. 4, no. 6, p. 497-501.

Hess, H. H., 1960, Stillwater igneous complex, Montana: Geol. Soc. Amer. Memoir 80, 240 p.

Ito, K. and Kennedy, G. C., 1968, Melting and phase relations in the plane tholeiite-lherzolite-nepheline basanite to 40 kilobars with geological implications: Contr. Min. Pet., v. 19, p. 177-211.

Kleeman, J. D. et al, 1969, Uranium distribution in ultramafic inclusions from Victorian basalts: Earth and Plan. Sci. Lett. v. 5, no. 7, p. 449-458.

Kushiro, I., 1969, Clinopyroxene solid solutions formed by reactions between diopside and plagioclase at high pressures: Min. Soc. Amer. Spec. Pub. No. 2, p. 179-191.

Laughlin et al, 1970, Sr-isotopic and chemical analyses of lherzolite inclusions and basalts, Bandera Crater, New Mexico (abs.): Trans. Amer. Geophys. Union, v. 51, no. 4, p. 449.

Leggo, P. J. and Hutchison, R., 1968, A Rb-Sr isotope study of ultrabasic xenoliths and their basaltic host rocks from the Massif Central, France: Earth and Plan. Sci. Lett., v. 5, no. 2, p. 71-75.

Nagasawa, H., 1969, Rare earths in peridotite nodules: Earth and Plan. Sci. Lett., v. 5, no. 6, p. 377-381.

Nixon, P. H. et al, 1963, Kimberlites and associated inclusions of Basutoland: Amer. Min., v. 48, p. 1090-1132.

Norman, J. C. and Haskin, L. A., 1968, The geochemistry of Sc: a comparison to the rare earths and Fe: Geochim. Cosmochim. Acta., v. 32, p. 93-108.

O'Hara, M. J., 1967, Garnetiferous ultrabasic rocks of orogenic regions, in Wyllie, P. J. (ed.), Ultramafic and Related Rocks, p. 167-172: New York, Wiley and Sons.

O'Hara, M. J., 1968, The bearing of phase equilibria studies in synthetic and natural systems on the origin and evolution of basic and ultrabasic rocks: Earth-Sci. Rev., v. 4, p. 69-133.

O'Hara, M. J., 1969, The origin of eclogite and ariegite nodules in basalt: Geol. Mag., v. 106, no. 4, p. 322-330.

O'Hara, M. J. and Yoder, H. S., 1967, Formation and fractionation of basic magmas at high pressures: Scott. Jour. Geol., v. 3, no. 1, p. 67-117.

Olcott, G. W., 1960, Preparation and use of a gelatine mounting medium for repeated oil immersion of minerals: Amer. Min., v. 45, p. 1099.

Rickwood, P. C. et al, 1968, A study of garnets from eclogite and peridotite xenoliths found in kimberlite: Contr. Min. Pet., v. 19, p. 271-301.

Shapiro, 1. and Brannock, W. W., 1956, Rapid analysis of silicate rocks: U. S. Geol. Surv. Bull. 1036-C.

Slavin, W., 1968, Atomic absorption spectroscopy: New York, Interscience, 307p.

Smith, J. V. and Gay, P., 1956, The powder patterns and lattice parameters of plagioclase feldspars, II: Min. Mag., v. 31, p. 744-762.

Sobolev, N. V. et al, 1968, The petrology of grospydite xenoliths from the Zagadochnaya Kimberlite pipe in Yakutia: Jour. Pet., v. 9, no. 2, p. 253-280.

Stueber, A. M. and Goles, G. G., 1967, Abundances of Na, Mn, Cr, Sc, and Co in ultramafic rocks: Geochim. Cosmochim. Acta., v. 31, p. 75-93.

Taylor, S. R. et al, 1969, Genetic significance of Co, Cr, Ni, Sc, and V content of andesites: Geochim. Cosmochim. Acta., v. 33, p. 275-286.

Watson, K. D. and Morton, D. M., 1968, Eclogite inclusions in kimberlite pipes at Garnet Ridge, northeastern Arizona: Amer. Min. v. 54, p. 267-285.

White, A. J. R., 1964, Clinopyroxenes from eclogites and basic granulites: Amer. Min., v. 49, nos. 7 and 8, p. 883-888.

White, R. W., 1966, Ultramafic inclusions in basaltic rocks from Hawaii: Contr. Min. Pet., v. 12, p. 245-314.

Winchell, H., 1958, The composition and physical properties of garnet: Amer. Min., v. 43, p. 595.

Wyllie, P. J., 1967, Ultramafic and related rocks in Ultramafic and Related Rocks: New York, Wiley and Sons, 464 p.

Yoder, H. S. and Tilley, C. E., 1962, Origin of basalt magmas: Jour. Pet., v. 3, p. 342-532.

York, D., 1966, Least-squares fitting of a straight line: Canad. Jour. Phys., v. 44, p. 1079-1086.

ACKNOWLEDGMENTS

The writer wishes to thank Drs. Ellis and Whitney of the Agronomy Department, Kansas State University, and Mr. O. K. Galle of the Kansas Geological Survey for providing facilities and assistance in the analytical chemistry.

Computer programs for the determination of chemical CIPW norms and Rb-Sr isochrons were provided by Dr. Charles Spooner.

The Research Corporation provided partial financial assistance. The Sr isotopic data were made possible by grants GA-317 and GA-10839 to D. G. Brookins.

The writer wishes to thank Dr. Brookins for his assistance during the preparation of this thesis. Thanks are also due Drs. Page Twiss, Sambhudas Chaudhuri, and N. Dean Eckhoff, committee members.

PETROGRAPHY AND GEOCHRONOLOGY OF BASIC AND ULTRABASIC INCLUSIONS FROM KIMBERLITES OF RILEY COUNTY, KANSAS

by

MICHAEL JOSEPH WOODS

B.A., University of Pennsylvania, 1964

AN ABSTRACT OF A MASTER'S THESIS

submitted in partial fulfillment of the

requirements for the degree

MASTER OF SCIENCE

Department of Geology and Geography

KANSAS STATE UNIVERSITY
Manhattan, Kansas

1970

Three ultrabasic nodules and three basement xenoliths from the Stockdale Kimberlite of Riley County, Kansas, were studied in detail by optical methods. Chemical analyses were also performed on the ultrabasic nodules and the clinopyroxenes from two of them by atomic absorption and flame photometry. In addition, Rb-Sr age data were gathered from the three xenoliths and one of the nodules.

Two of the nodules are plagioclase and garnet bearing pyroxenites believed to be of upper mantle or possibly lowermost crustal origin. Evidence to support such a conclusion consists primarily of a garnet-orthopyroxene-spinel-sapphirine-kyanite assemblage in one of the samples. Work by a number of authors suggest that such an assemblage indicates a minimum pressure of about 13.5 kilobars, which corresponds to the continental crust-mantle boundary. The jadeite:tschermakite ratio of clinopyroxene from the same nodule is about the same as the lowest ratios reported for eclogite clinopyroxenes, suggesting that the nodule may reflect conditions transitional between the eclogite and granulite facies. Further evidence along this line is the composition of garnet from the same nodule, found typical of garnet compositions from eclogite nodules in African kimberlites.

The second pyroxenite is clearly of granulite grade, based on the jadeite:tschermakite ratio and garnet composition. Both pyroxenites are believed to have formed as precipitates from melts, based on textural relations.

The third ultrabasic nodule is an eclogite, consisting of omphacite and garnet. Quartz and rutile are apparently present

in very minor amounts. Textural evidence suggests that the garnet is of secondary origin, having formed from the clinopyroxene.

The basement xenoliths studied consist of two hypersthene gabbros and one diorite. Rb-Sr data provide dates of 82 ± 25, 692 ± 108, and 1585 ± 95 m.y. respectively. The granulite pyroxenite nodule gives a date of 240 ± 8 m.y. Most of these data are believed to indicate the time of the latest thermal event, rather than the time of formation. The date for the diorite may be an exception.